Copyright Warning & Restrictions

The copyright law of the United States (Title 17, United States Code) governs the making of photocopies or other reproductions of copyrighted material.

Under certain conditions specified in the law, libraries and archives are authorized to furnish a photocopy or other reproduction. One of these specified conditions is that the photocopy or reproduction is not to be "used for any purpose other than private study, scholarship, or research." If a, user makes a request for, or later uses, a photocopy or reproduction for purposes in excess of "fair use" that user may be liable for copyright infringement,

This institution reserves the right to refuse to accept a copying order if, in its judgment, fulfillment of the order would involve violation of copyright law.

Please Note: The author retains the copyright while the New Jersey Institute of Technology reserves the right to distribute this thesis or dissertation

Printing note: If you do not wish to print this page, then select "Pages from: first page # to: last page #" on the print dialog screen

ABSTRACT

AUTOMATED MULTI-WELL NEURAL INJURY DEVICE

by
Linda Y Chen

Traumatic Brain Injury (TBI) is a wide spread pathological problem occurring in 1.4 million individuals every year according to the National Institute of Neurological Disorders and Stroke. There are several types of TBI and the most prominent ones are concussion, contusion, hematoma, coup-contrecoup injury and diffuse axonal injury (DAI). The most severe type and the one that is the hardest to diagnose is DAI. DAI occurs mostly due to accidents relating to automobile, motorcycles and in some cases fall and assault, resulting in a "shearing" phenomenon of the brain. Patients with DAI can range from being, mildly injured, severely disabled or result in death.

This current research is focusing on creating a neural injury device for a twenty four well apparatus with an easy to use software based control. This neural injury device used air pressure to create blast injury to the neural cells in a uniaxial direction. This thesis research focused on the software design for controlling the neural injury device. Several experiments was performed to verify its efficiency in creating consistent, accurate and controllable injury to 24 well of cultured neurons. The results from the experiments demonstrate that this automated multi-well neural injury device is very reliable in terms of controllability, accuracy and consistency.

AUTOMATED MULTI-WELL NEURAL INJURY DEVICE

by
Linda Y Chen

A Thesis
Submitted to the Faculty of
New Jersey Institute of Technology
in Partial Fulfillment of the Requirements for the
Degree of Master of Science in Biomedical Engineering

Department of Biomedical Engineering

May 2008

APPROVAL PAGE

AUTOMATED MULTI-WELL NEURAL INJURY DEVICE

Linda Y Chen

Dr. Bryan J Pfister, PhD, Thesis Advisor — Date
Assistant Professor of Biomedical Engineering, NJIT

Dr. Tara L. Alvarez, PhD, Committee Member — Date
Assistant Professor of Biomedical Engineering, NJIT

Dr. George Collins, PhD, Committee Member — Date
Research Professor of Biomedical Engineering, NJIT

Dr. Maximillian Roman, PhD, Committee Member — Date
Director of Masters Program, NJIT

BIOGRAPHICAL SKETCH

Author: Linda Y Chen

Degree: Master of Science

Date: May 2008

Undergraduate and Graduate Education:

- Master of Science in Biomedical Engineering,
  New Jersey Institute of Technology, Newark, NJ, 2008

- Bachelor of Science in Biomedical Engineering,
  Rensselaer Polytechnic Institute, Troy, NY, 2006

Major: Biomedical Engineering

I would like to dedicate this thesis
to my family for providing me with
much needed support during the
course of my studies in NJIT.

ACKNOWLEDGMENT

I would like to express my gratitude to my thesis advisor, Dr. Bryan J. Pfister for giving me the opportunity to participate on this research. He had given me much needed help and insight in further improvement to every aspect of the design in this research. He was a very valuable source of expertise that I had to rely on tremendously. Additionally, I would like to thank Dr. Richard Foulds for providing me with much help throughout the course of this research, especially in the software control aspect. In addition, I would like to thank Dr. Maxmillian Roman for providing me with much needed help in understanding the flow dynamic of air going into the apparatus and how to go about it to get a more uniform air distribution within the injury apparatus. Furthermore, I would like to extend my thanks to Dr. Pfister, Dr. Roman, Dr. George Collins and Dr. Tara Alvarez for participating in my defense committee, providing me with my new approaches and ideas to improving the Automated Multi-well Neural Injury Device.

Furthermore, I would like to thank the New Jersey Commission on Brain Injury Research for their support with funding much of the instruments and parts required for this project. These equipments are essential components for moving this project forward.

Many of my fellow graduate students in the CHEN building laboratory are deserving of recognition for their support. I also wish to thank Yi Guo for his assistance over the course of this project providing much help in the control program, his expertise is invaluable. Additionally, I would like to thank Marko Grbic with his assistant in the hardware connections and injury apparatus design.

TABLE OF CONTENTS

TABLE OF CONTENTS
(Continued)

LIST OF TABLES

LIST OF FIGURES

CHAPTER 1

INTRODUCTION

1.1 Objective

The objective of our laboratory's research is to create an automated multi-well neural injury device that is able to produce a predetermined dynamic pressure pulse to a 24 well neural injury apparatus accurately and consistently. This pressure delivers a sudden insult, stretching the silicone causing sudden injury to the neural cell, mimicking the deformations of a traumatic brain injury (TBI). The control of the neural injury device is software based using Labview 8.0. It will allow the user to specify an input pressure and a solenoid valve opening time to adjust the pressure pulse dynamic for injuring the neural cells are cultured on the silicone membrane. This thesis focuses on the development and testing of a control program essential to regulating the pressure pulse going into the injury apparatus. The program will sought to demonstrate that it can adjust the pressure driving force and timing of the valve to control the pressure wave recorded by the pressure transducer.

This device has the capability of sending in a programmable minimum pulse width of 5 millisecond (ms), 1 ms sensitivity, to control the solenoid valve to release air into the injury apparatus. There will be four tests performed to determine the efficacy of this device's control at the specific resolution. The first objective the control program is accuracy and consistency of the injury pressure pulse; therefore a test of repeated measurements will be conducted.

The second test will seek to determine the dynamic control limits or capability of the device due to both volume and valve timing. A dummy apparatus of equivalent

volume to the actual injury apparatus will be tested with the same pressure and time parameters. The purpose is to determine the affects of volume and valve response limitation connected to the device. This is done to assess the effect these varying parameters will have on the driving force of air pressure going into the injury apparatus. Additional testing will be conducted to determine whether volume contributes to the pressure rise time and peak pressure.

The third test performed to assess the repeatability or consistency in the device control using the program. Measurements will be made in one location to indicate that 3 or more consecutive pressure pulses are identical.

Finally, the program will determine the consistency of the pressure pulse in 9 different measurement locations. This will give insight into the dynamics of the pressure wave. The goal is to illustrate that all 24 wells reach peak pressure at the same time interval. Ultimately, these tests will indicate whether the device is capability of pressurizing the injury wells to 7 psi in 5 ms.

1.2 Background Information

The study of damage to neurons during an onset and progression of a traumatic brain injury (TBI) is significant in the development of more efficient diagnostic, treatment and preventive measures to decrease the rate of morbidity and mortality due to such injuries. According to Centers for Disease Control and Prevention (CDC), 1.4 million people have had experienced TBI each year and 50,000 of those died from their injuries [6]. The leading cause for TBI ranges from falls, motor vehicle accidents to assaults [6]. Additionally, blast head injury is another major cause of TBI and it is a very common result for those involve in combat and approximately 88% of military personnel who are

involved are inflicted with such injury due to explosive devices or mortar [21]. Even though death from TBI only occurs in less than 1% of those populations, the side effects from such injuries can range from mild to short term and long term disability [7]. The age that are most affected by TBI are in the range of 15 to 45 years old, the most productive years in an adult life [7]. As a result, TBI is becoming a prominent socio-economic problem; therefore research in the study of blast injury of neural cells is important in gaining a better understanding of the TBI [7].

There are several types of TBI and some of these include diffuse axonal injury (DAI), concussion, contusion, hematoma, coup-contrecoup and whiplash. These injuries can be classified as either diffuse or focal trauma to the central nervous system (CNS) [2]. The most common injury is DAI, occurring in almost 50% of patients with a severe TBI [8]. In DAI, the damage affects the entire brain region due to the rapid motion of the brain upon impact; therefore, the damage will appear homogenous and often very difficult to detect under normal radiological examination, whereas in focal impact the site of injury is often very prevalent and this is illustrated in Figure 1.1.

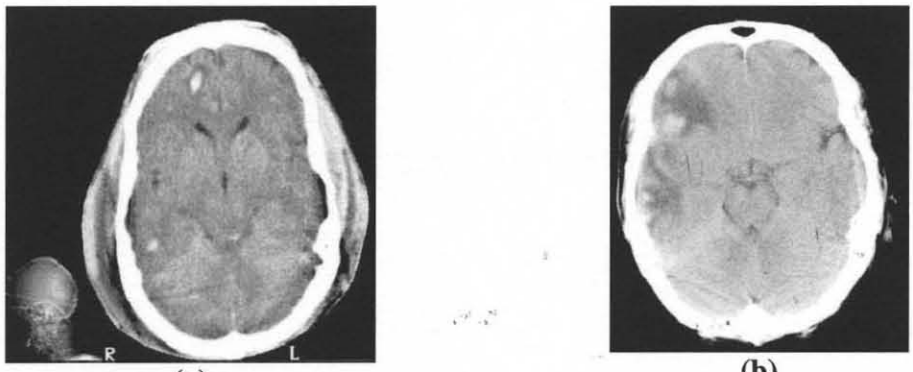

(a) (b)

Figure 1.1 (a) CT image of a diffuse axonal injury of the brain. (b) CT image of a focal brain injury, specifically brain contusion. [23]

In DAI, lesions tend to be multiple and small and the common sites include the corpus callosium, the gray matter-white matter junction in parasagittal areas, the deep

periventricular white matter, the basal gangia and internal capsule, the hippocampal and parahippocampal regions, the dorsolateral aspect of the brainstem, and the cerebellum [8].

In diffuse brain trauma the neural cells undergo inertial loading due to rotational acceleration and deceleration motion, as exhibited from Figure 1.2, where the shearing force is exerted perpendicular to the axis of rotation of the brain [2, 7].

Figure 1.2 Rapid rotational acceleration/deceleration of the head of a pig in the coronal plane [2].

These inertial loading encompassed dynamic shear, tensile, and compressive strains during tissue deformation [2]. Since the brain tissues are of viscoelastic nature, it has the potential of undergoing rapid uniaxial stretch, elongating the neurons causing damage to the axonal cytoskeleton [2, 9-11]. In the past, biaxial stretch had been used as an *in vitro* model for neural injury to demonstrate TBI [18], but neurological experiments had indicated that the neurons actually deformations are unidirectional, therefore uniaxial stretch is clinically accepted [1, 18].

Furthermore into the mechanics of neural injury, the applied force to the brain during a TBI occurs in less than 50 milliseconds (ms) and the severity of the axonal injury is dependent on both magnitude of strain and rate of strain [2, 11]. Based on experimental findings, it had suggested that strains between 0.10 and 0.50 with a strain rate of 10-50s^{-1} were necessary to produce damage to neurons in a physical model [5, 14-

17]. Therefore, an *in vitro* system that allows more insight into these cellular events will enable a better understanding of the different types of brain injuries.

In the past, there are researches done to gain a better understanding of brain injury via an *in vitro* model using rat brain tissue slices and use a pendulum to induce an impact to the neural tissue [13]. However, this types of model is difficult to do an accurate measurements to assess the extend of the cellular deformation to give an accurate strain and strain rate [13]

In the Penn Model, which is the neural injury device being used in the University of Pennsylvania, it is able to replicate a wave sequence deformations from large head rotations such as falls or automobile accident. The design of the Penn Model consisted of an aluminum cover block, a stainless steel plate, and an air pulse-generating system [19]. In addition, it contains solenoid valves and pressure transducer which is controlled by an analog-to-digital board through a computer for driving the system and providing feedback [19], Figure 1.3.

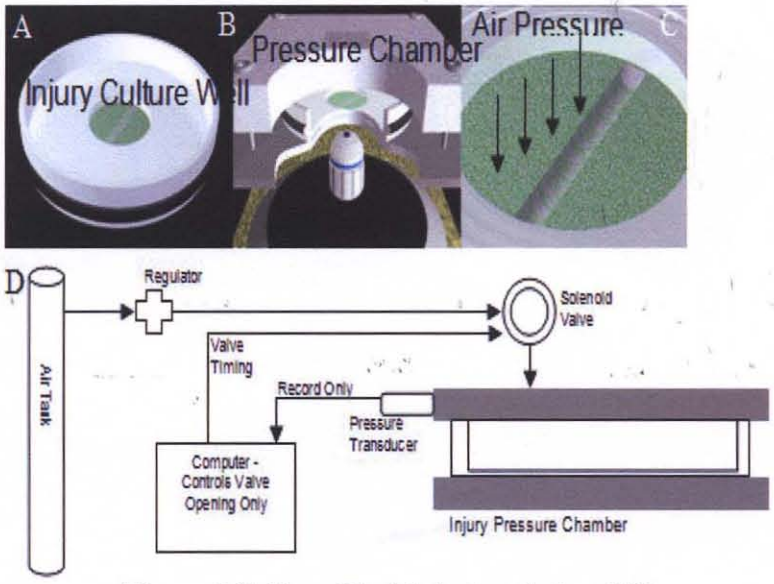

Figure 1.3 Penn Model device design [19].

The Penn Model is able to produce a pressure vs. time curve as showed in Figure 1.4 [3].

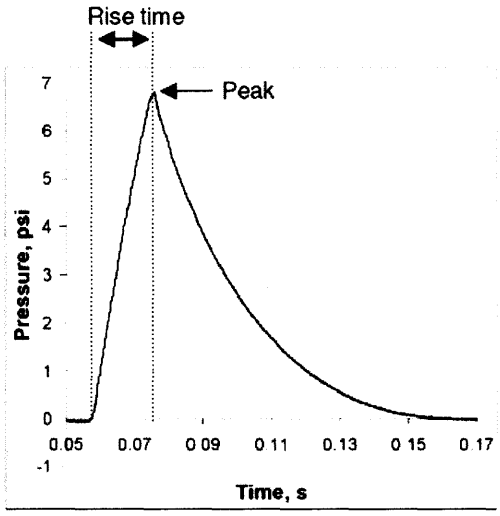

Figure 1.4 Pressure pulse produced by the Penn Model [3].

The result illustrated the pressure produced during an onset of a head trauma which is represented by the "rise time" and the "peak" is the highest point of impact [3]. The peak pressure is the point of indicative of the applied strain, where the maximum stretch of the neural cells occurred. This curve is the representation of a TBI, in which the pressure is what induced the traumatic impact to these cells within a matter of 20 ms at an input pressure of 40 psi. It produced a strain of 0.65 and strain rate at $15s^{-1}$[5].

The automated multi-well injury device uses a similar concept made by the Penn Model where air pressure will be the injury mechanism. However, there are several improvements in which the automated multi-well injury device will implement. These improvements include a software based control platform and an injury apparatus that supports 24 wells of cultured neurons. Additionally, this neural injury device will sought to achieve a similar peak pressure as the Penn Model, but at a lower time interval. Figure 1.5 is a schematic of an overview of how the multi-well neural injury device will operate. Mridusmita Choudhury's thesis research had focused on the design of the injury apparatus so that air pressure can distribute evenly during the neural injury process [24].

In this design, it incorporates a silicone membrane as part of the 24 well for cell culture plate. This 24 well cell culture will be put into the injury chamber, which composed of two aluminum enclosures that tightens with a screw and nut mechanism. The cells that are cultured on to the silicone membrane will stretch under pressure and this stretch creates the neural injury similar to that of TBI. Now the next phase of the research will focus on refining the control program to induce the desire pressure within the injury apparatus with accuracy, consistency and repeatability.

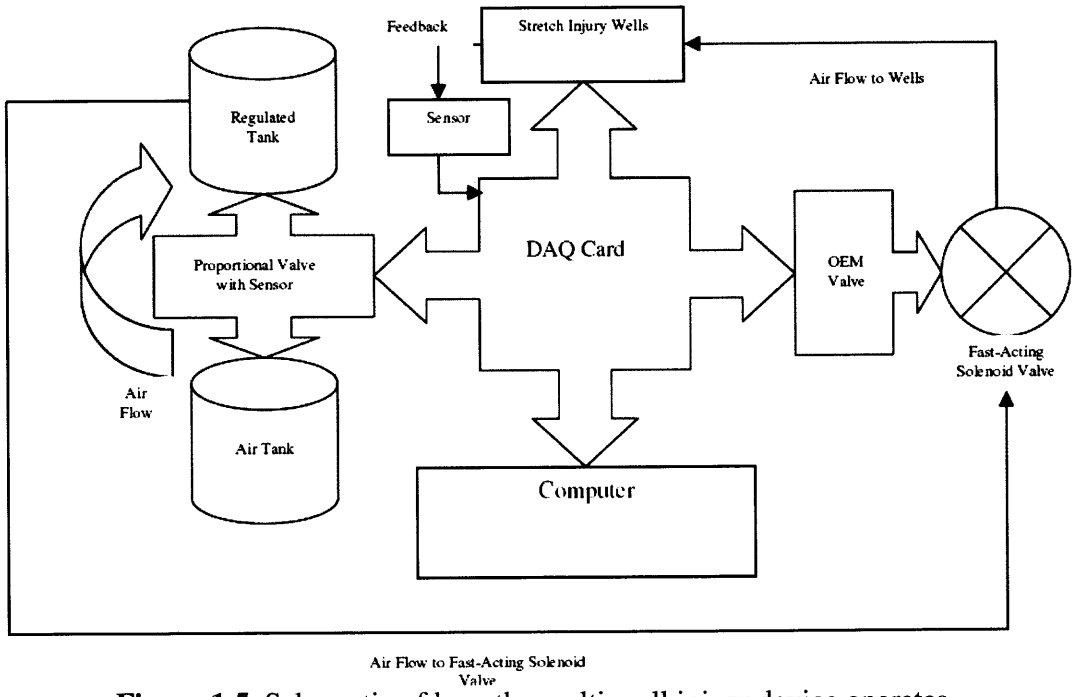

Figure 1.5 Schematic of how the multi-well injury device operates.

CHAPTER 2

MATERIALS AND METHODS

In Chapter 2 the materials and methods involved in the design of the software control of the multi-well injury device will be presented. There will be two parts to designing the control component to induce pressure to the injury apparatus. The first part is the hardware design and the second part is the software control design.

2.1 Hardware Components

There are six main components to the neural injury device, the VSO-EP electronic pressure control unit (Parker Hannifin Corporation, Pine Brook NJ), OEM valve driver (Parker Hannifin Corporation, Pine Brook NJ), the Series-9 3-way fast-acting solenoid (Parker Hannifin Corporation, Pine Brook NJ), the EPX pressure sensor (Entran Sensor & Electronics, Fairfield NJ), the IAM amplifier (Entran Sensor & Electronics, Fairfield NJ), and the NI PCI-6024e data acquisition (DAQ) card (National Instruments Corp., Austin TX). These major components are either power by a 15 Volt (V) or 24 V power sources (DigiKey, Thief River Falls MN). The full hardware schematic of these devices is shown in Figure A.1 of the appendix.

The VSO-EP electronic pressure control unit is responsible for the transfer of air pressure to the regulated (reserved) tank which serves as the driving force for pressurization of the actual injury apparatus. The purpose of this device is to maintain a consistent input pressure, creating an initial driving force to move air into the injury apparatus. This specific valve has the capability to ensure high accuracy in gas flow due

to its internal closed loop control and external sensor pressure capability. This proportional valve has a pressure sensitivity of 2.713% ± 0.672 and a reproducible sensitivity of 0.482% +/ -0.217. In addition it is able to control up to 100 psi of air pressure. This device will be controlled via the NI PCI-6024e DAQ card and BNC 2090 break out box, connecting to the feedback analog pin AI 0 and the control output analog pin AO.0. The DAQ card will initialize the valve by input of a voltage signal and will consistently maintained throughout the injury process. The voltage signal sent to the VSO-EP corresponds with a specific pressure; at 1 V, it will equate to 20 psi, creating a linear curve (Figure 2.1).

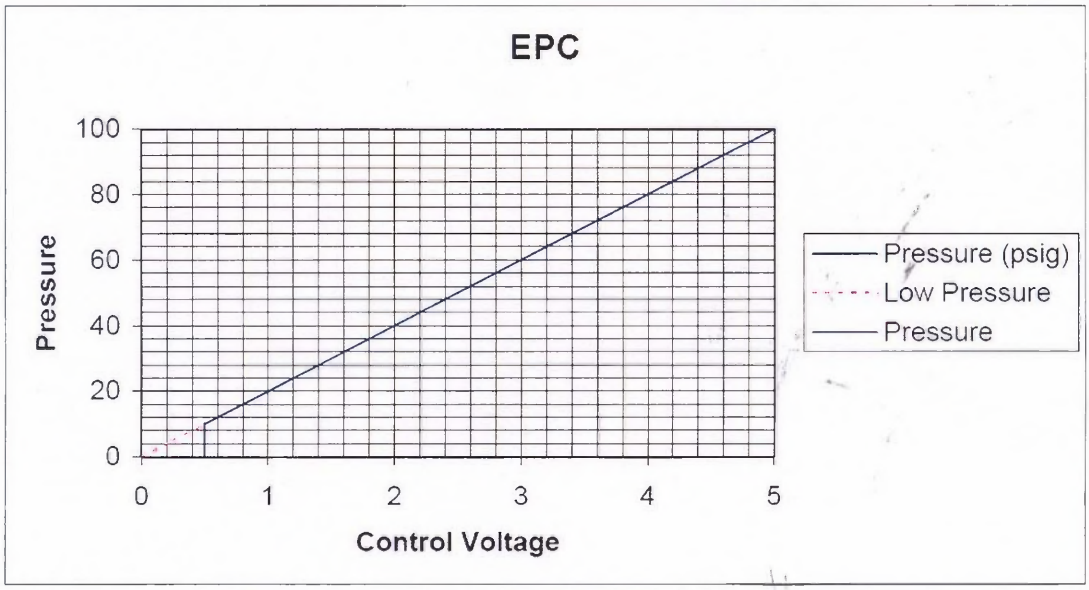

Type 2: 0-5 volts = 0-100 psig.

Figure 2.1 VSO-EP Proportional valve performance specification curve.

The Series-9 3-way fast-acting solenoid valve provides high speed air flow through a 0.116 inch orifice to the neural injury apparatus in addition to a relieve valve for depressurization of the injury apparatus. It has a response time of 5-7 ms and offers repeatability and consistency and can handle up to 250 Psi of pressure. The OEM valve driver sends an input voltage to the series 9 3-way fast-acting solenoid valve by moving

its jumper block [20]. The valve driver is driven by a 5 V on board output signal, supplying a 24 V to open up the series 9 solenoid valve. It has the capability of selecting the hold-in voltage to supply to the valve coil [20]. Therefore, voltage to the valve coil is independent of the supply voltage [20]. The control of this driver will be done by connecting pin J1.2 to the analog output channel on the DAQ card, acting as a switch to trigger activation.

According to the data from the Penn model, as shown in Figure 1.3, approximately 7 psi is required to induce silicone deformation; cells cultured on the silicone will stretch causing injury to the cytoskeleton of the neural axon. Based on the calculations from the Bernoulli Equation for incompressible air flow for a solenoid valve with an orifice size of 0.116 inches in diameter, with an initial pressure of 80 psi, it is able to produce a pressure a 7 psi within 5 ms for all 24 wells (Figure B.1). The equation used is as follows:

$$Q = \sqrt{\frac{\pi^2 (P_1 - P_2)(D_1^4 - D_2^4)}{16\rho}}$$

Figure 2.2 Flow Equation Derived from Bernoulli Equation, Refer to Figure B.

The variables P_1 and P_2 define initial and final pressure, Q is the flow rate, ρ is the density of air, D_1 is the diameter of the tubing and D_2 is the orifice size. For details of the derivation of this equation and calculations of flow rate, refer to the Appendix, Figure B.1. Since the only unknown variable is the flow rate, which is important in figuring out when it will be able to reach a volume of 5.80 in^3, which is the exact volume of the all 24 wells with the recess space, calculation of this volume is illustrated in the Appendix, Figure C.1, for air flow. According to the calculation performed in Figure B.1, at the initial pressure of 80 psi, it is able to fill up a volume of 6.03 in^3. Thus, by changing the

initial pressure and its corresponding valve opening time, the strain and strain rate can be accurately controlled.

A pressure sensor, EPX, was used to provide feedback monitoring of the pressure in the neural injury apparatus. It has an output voltage of 0V to 50 mV for indication of pressure changes within the apparatus, with a sensitivity of +1/+2% with a ±50 mV maximum out signal. The IAM amplifier will take in these signals, provided by the EPX pressure sensor, and amplified it to a signal range of 0 to 12 VDC, using a gain of 201.8, in order for the DAQ card to read it.

All these major components are controlled via the NI PCI-6024e DAQ card, providing a semi-close loop system in which it requires its user to adjust its inputs, reserve pressure and valve timing, after each test run to get the desire rise time and peak pressure. It is capable of monitoring feedback and controlling each component by using the software program in LabView 8.0. It is also capable of analog-to-digital or digital-to-analog conversions enabling ease of control and real-time feedback monitoring.

2.2 Software Control Component

The software control provides a bridge that brings all the hardware components together into one working unit. The software control instructions are written using National Instrument's Labview 8.0 development system. This software package enables users with the flexibility of creating control and embedded design applications. In this section the design concept of the program will be discuss.

In general, the software part of this device has three major parts, controlling input pressure to the reserve tank, releasing the air from the reserve tank to the injury apparatus and the data acquisition. The controlling of the input pressure to the reserve tank is based

on the VSO-EP's external sensor and internal loop. The sequence of the control program will first (1) use the input voltage by the user, corresponding to the desired pressure, to fill the reserve tank, then (2) then the OEM valve will activate via analog output of 5V to pin J1.2 and (3) data from the EPX transducer feedback will start collecting 20 ms prior to series 9 valve activation and start collecting until the injuring process ends. This is how the current control program is designed.

A control program was made that has very similar control algorithm as the current control program. The difference between the two programs was that one is software based timing (Figure E.1) and the program that uses the NI PCI-6024e DAQ card employs hardware based timing (Figure F.1-3). The advantage between hardware based timing and software based timing is that hardware timing bypasses the CPU processor interference, creating a more accurate timing control. As a result, hardware timing is the prefer method to use for this device; that is why the NI PCI-6024e is used instead of the NI USB-6009.

CHAPTER 3

IMPLEMENTATION and ANALYSIS

This chapter will focus on the implementation of the software control program to obtain data to give a good assessment of the automated multi-well neural injury device. The collected data will be analyzed using the Minitab software. The types of data will be described in the following sections, in addition to the specific statistical analysis employed.

3.1 Software Operation

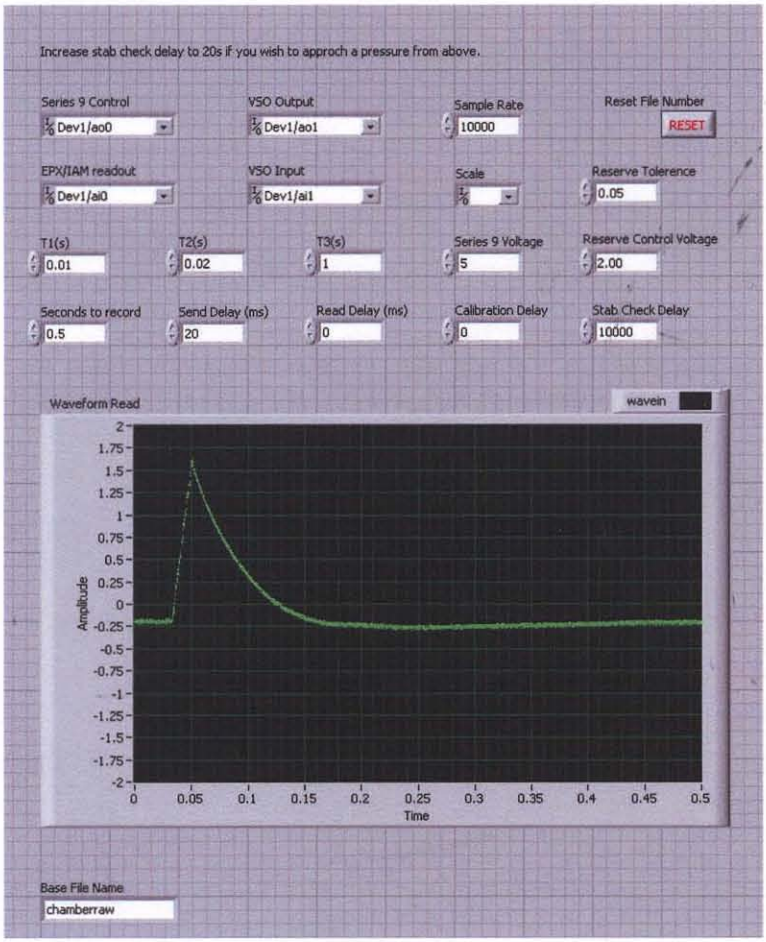

Figure 3.1 Front panel of the software control program.

The are three important parts that are essential to the software control operation were regulation of the proportional valve to pressurize the reserve tank, controlling the valve opening time of the solenoid valve to release air into the injury apparatus and data acquisition for analysis. The user will enters in a specific input pressure under "Reserve Control Voltage" and the valve timing for the series-9 under "T2". These input controls are indicated in Figure 3.1. As the program is initialized, it will first fill the reserve tank to the pressure indicated by the input voltage, in this case 2 V = 40 psi, and it is being controlled by the subVIs shown in Figure 3.2.

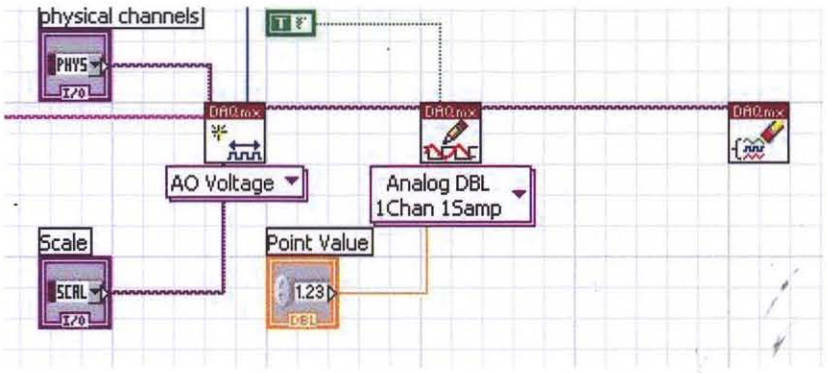

Figure 3.2 Reserve control voltage.

The physical channel ao1 produces a control signal to the proportional valve to control air into the reserve tank; it undergoes a close loop to maintain the specify pressure level. This channel can be changed via the front panel under "VSO-EP Output" in Figure 3.1. The way the signal is being send to the VSO-EP using DAQmx functions where the DAQmx Create VI (Virtual Instrument) defines the channel type used. In this case it is AO Voltage, indicating that it is an analog output control using the physical channel ao1, Figure 3.2. After creating a physical channel, it will wired to the DAQmx Write VI, where it will define the type of signal generation, the number of virtual channels, the number of samples and the data type to be selected. The signal going to the VSO-EP will

be an analog double precision floating point numeric as indicated by "DBL" for a one channel one sample output. The "Reserve Control Voltage" input is wired to the "Point Value" input control associated with the VSO-EP Reserve Control VI shown in Figure 3.2.

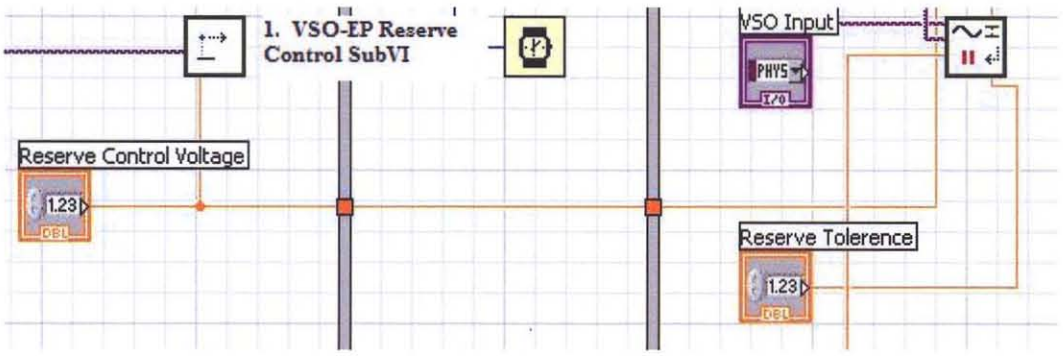

Figure 3.3 VSO-EP reserve control subVI used in injury control VI.

Once the input voltage had been set, it will fill the reserve tank with air until it reaches the pressure associated with the input voltage via control of the while loop shown in Figure 3.4. The "Reserve Control Voltage" (Figure 3.3) is wired to "Command Voltage" (Figure 3.4) so that the feedback signal from the VSO-EP (channels ai1, Figure 3.1) will continuously check the difference between them until it is less or equal to the set tolerance of 0.05 (Figure 3.4). When this conditioned is met, the program will exit the while loop and move on to the next stack sequence or next step. The next step will be the release air into the injury chamber or apparatus via the solenoid valve. Prior to discussing the series 9 valve control for air release into the injury chamber, assuming that the injury process had ended, Figure 3.5 illustrates the end of task for VSO-EP control.

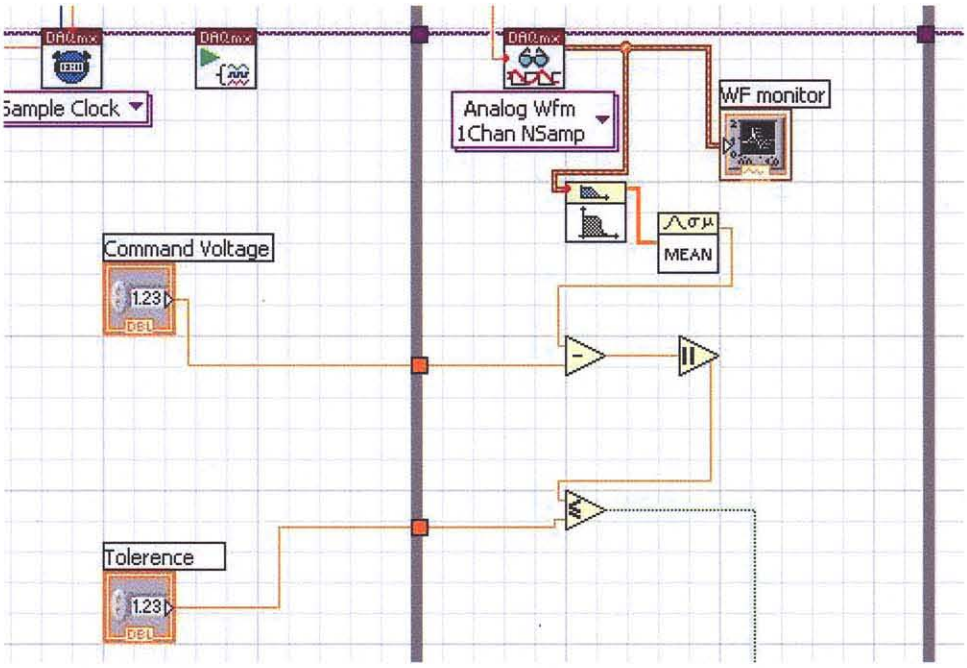

Figure 3.4 VSO-EP software feedback control.

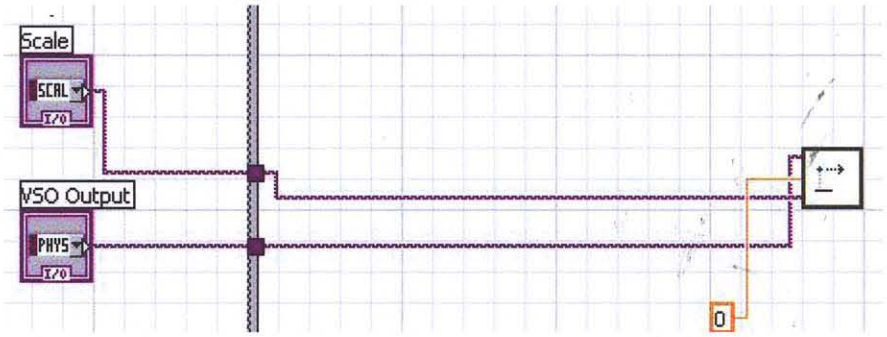

Figure 3.5 Indication of end of task for VSO-EP.

The next step in the control program after the VSO-EP had filled the reserve tank with the specify pressure is to create a pulse wave signal to the buffer of the DAQ prior to trigger the solenoid valve. By using hardware timing, the CPU is bypassed, and will initial the task with high accuracy. In Figure 3.6 it is a VI that regulates this process.

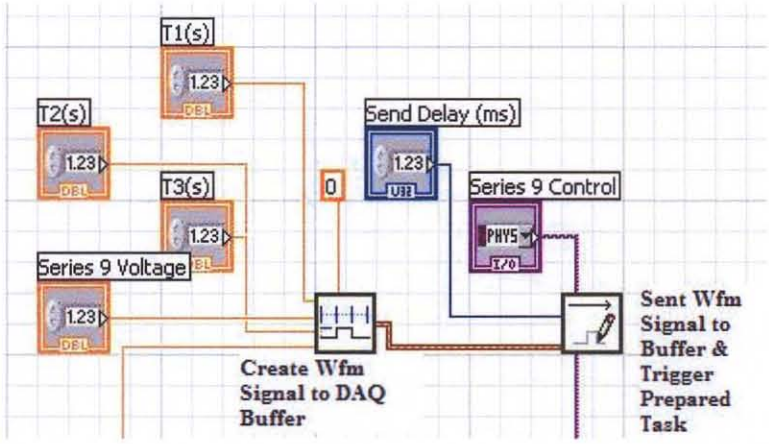

Figure 3.6 Series 9 valve control for air release into the injury apparatus.

In Figure 3.6 the T1, T2 and T3 indicates the start of the period at 0V (T1), the pulse duration at 5V (T2) and pulse duration at 0 V (T3). T3 is set to 1 second to set the timing to complete air release with the injury apparatus to obtain the downward slope, whereas T2 is responsible for the length of time the series 9 valve remains opens.

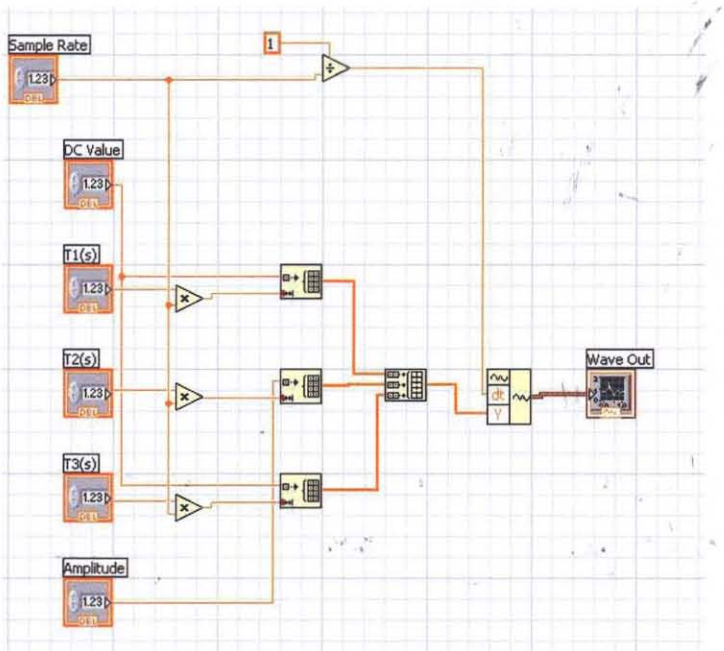

Figure 3.7 Building a waveform signal using array.

In Figure 3.7 the pulse wave is created using a series of array wiring it to the Create Waveform function where "dt" channel indicates the timing resolution at 1 ms and the

T1, T2 and T3 array is wired to the "Y" channel to form the pulse wave. The "Wave Out" indicator will be set as an output variable and wired to the sendwave VI to initiate the task of air into the injury apparatus (Figure 3.8).

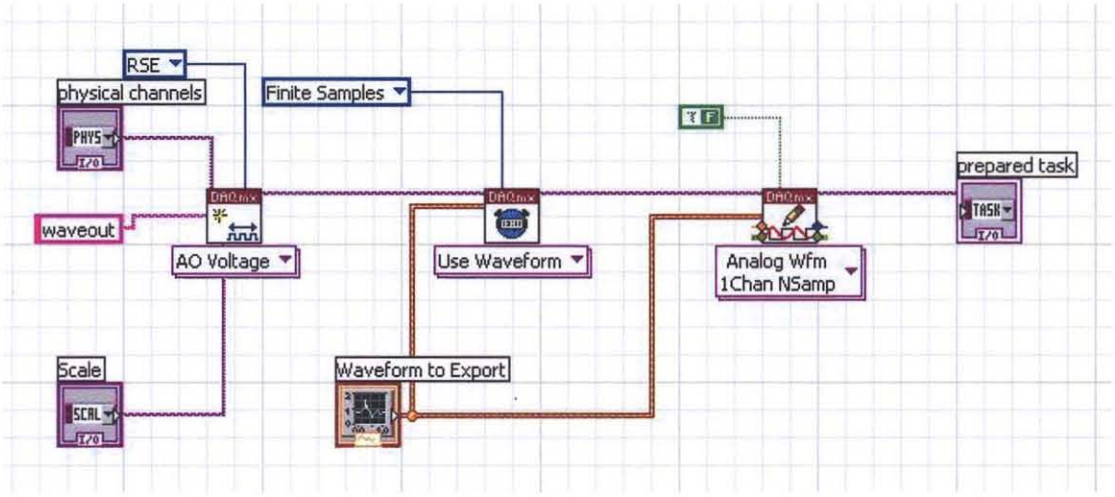

Figure 3.8 Sendwave VI for downloading pulse wave to DAQ buffer and initiating task.

In the sendwave VI, an analog channel is created, ao0, and is wired to the Timing VI, which sets the rate of the output control (Figure 3.8). The pulse wave is wired to the DAQmx Write VI, sending in voltage for T1, T2, and T3 periods (Figure 3.7), where DC value is set to 0V and Amplitude is set to 5V. When the injuring process is ready to begin, the control program will trigger the ao0 analog channel to release the instruction already stored in its hardware buffer (Figure 3.9)

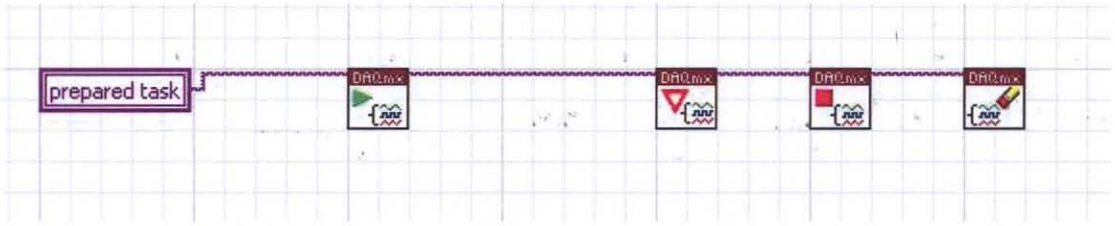

Figure 3.9 Triggering task stored in hardware buffer.

Data collection begins 30 ms before the initiation of the task associated with opening of the series 9 solenoid valve. In Figure 3.10 it creates the analog feedback channel, ai0, and the feedback signals are stored in the DAQ buffer.

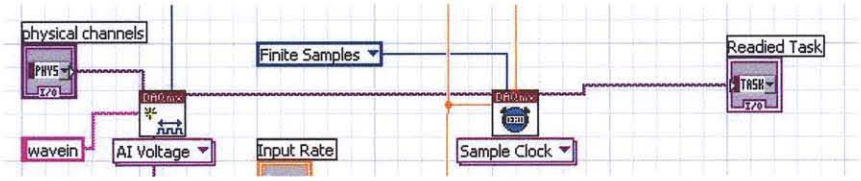

Figure 3.10 EPX sensor feedback setup prior to outputting into external file.

After the EPX sensor finishes collecting the data, these signals will be output to a data file illustrated in Figure 3.11.

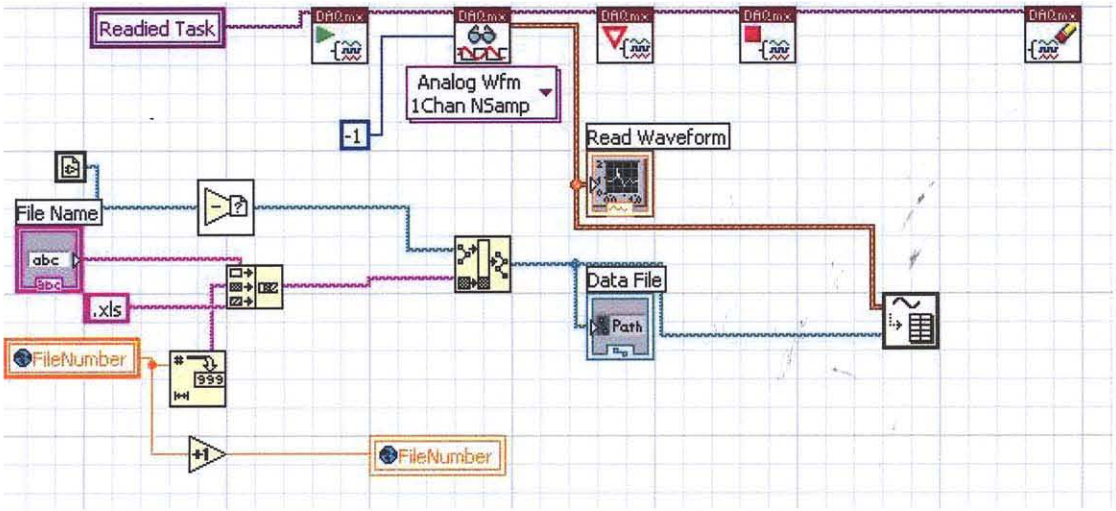

Figure 3.11 Data acquisition from the DAQ buffer.

The DAQ sent in the feedback information through the channel in which the data was collected from and stored in a Microsoft Excel file. In the following section, it will evaluate both the control program operation and injury apparatus design based on a series of experiments done to assess the overall performance of the Automated Multi-well Neural Injury Device.

3.2 Experiments to Evaluate the Control Program

After the completion of the software program via LabView, pressure pulse data will be collected with varying input pressure and valve timing for analysis of the change in rise time and peak pressure. The two main parameters that will be responsible for adjusting the output pressure to the injury apparatus is the input voltage for the reserve tank and the timing interval indicated as T2 in the front panel (Figure 3.1) of the control program.

The feedback from the external sensor of the VSO-EP is used as the basis for converting the EPX sensor feedback to its corresponding pressure in psi. As pressure goes through the VSO-EP valve, the relationship between the voltage and pressure is linear. At 1 V, the pressure output is 20 psi. Since the VSO-EP has its own internal closed loop system, it is able to maintain the specified pressure for any time frame. Therefore, by knowing what the pressure is in a close apparatus using the VSO-EP, one can use it to define the pressure for the EPX transducer; this method is to calibrate the EPX.

There will be several sets of data collected using this software program. The first of which would be to illustrate the capability of the series 9 solenoid valve to evaluate how fast it is able to open and close, releasing air into the injury wells. The expected pulse width will be programmable down to 5 ms with adjustment steps of 1 ms. Data will be collected at a constant pressure of 90 psi, and the opening time of the series-9 solenoid valves will be decreased from from 15ms to 1ms. In this test, both the dummy volume and the actual injury apparatus were used. The dummy volume is based on the volume of the 24 injury wells with a 0.1 inch recess space at the top of the apparatus as illustrated in Figure 3.12.

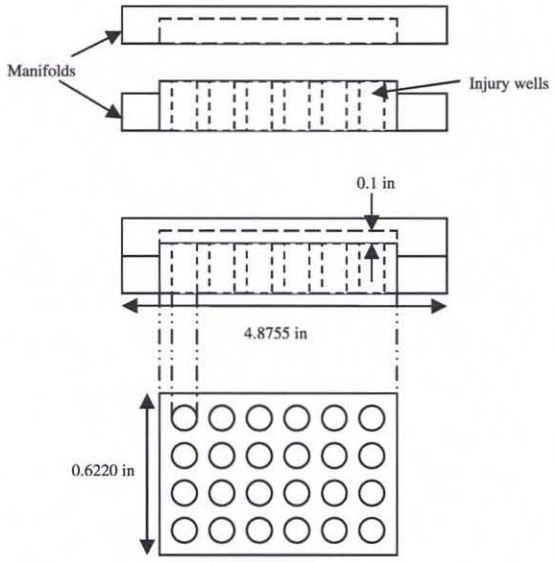

Figure 3.12 Injury Apparatus with a 0.1 in recess space.

The dummy volume setup is based on 2 inch tube leading into the apparatus (Figure 3.13), eliminating much of the obstructions poses by the multiple tubes leading into the actual 24 well injury cell culture dish.

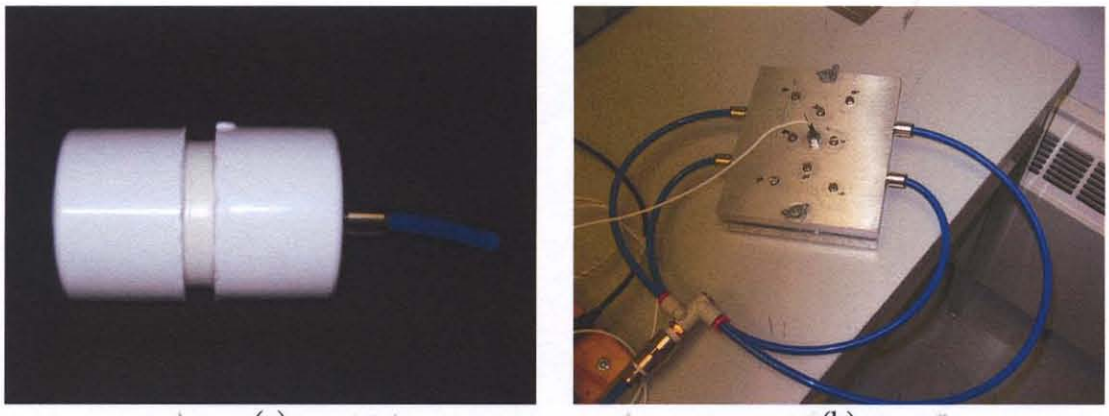

(a) (b)

Figure 3.13 (a)Dummy volume and (b) Injury Apparatus.

The second evaluation will be on consistency and repeatability rise time and peak pressure at a specific time interval. Peak pressure data will be collected consecutively to obtain 10 sets of samples, at the same input reserve pressure and time parameters. Statistical analysis will be used to determine the variance among each of the maximum

points from each data set. The maximum point is indicative of the peak pressure inside the injury apparatus. Additionally, graphical indication will illustrate consistency in both rise time and peak pressure.

The third test that will evaluate the parameters which contribute to the maximum air pressure reach in the injury apparatus. Since there is more tube in the actual injury apparatus as compared with the dummy apparatus, the volume in which the air had to pass through to get to the actual injury apparatus had increased. This might contribute to a decrease in driving force of air into the injury wells. The amount of tubing going into the injury apparatus and the volume of the apparatus are important parameter to the overall design of the injury apparatus to ensure optimum performance. Since the dummy apparatus contains the same volume as the actual injury apparatus, it will be used to test whether air flow exposure to more surface area leading to the injury wells will alter its driving force. There will only be one short tube going into a closed volume, dummy apparatus, with the EPX transducer attached to the other end (Figure 3.13a). Data will be collected for both dummy and multi-well apparatus to compare air flow dynamic for each of the setup.

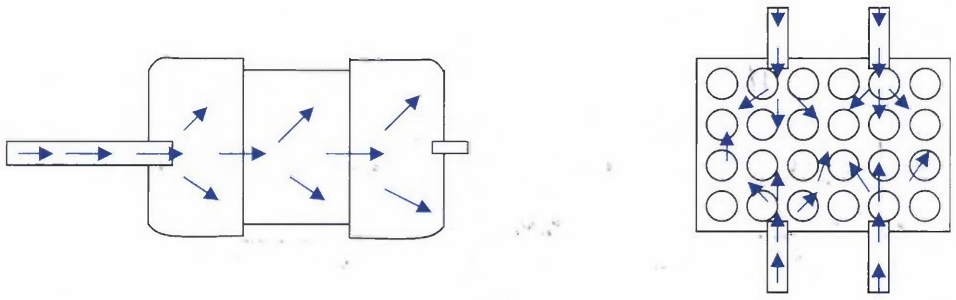

(a) (b)

Figure 3.14 Mocked up flow Dynamics of air for the (a) dummy volume and (b) the injury apparatus.

Since the setup (Figure 3.14) is different between the two apparatus of the same volume, the flow dynamic likely varies in terms pressure distribution within the pressure chamber

as shown. The reasonable estimation of the flow dynamics between the apparatuses shown in Figure 3.14, Figure 3.14a will reach pressure equilibrium faster than Figure 3.14b. In Figure 3.14b, there should be a slight pressure variation within the corner area of the 24 wells plate and the midsection of the apparatus will reach the equilibrium pressure at a faster rate.

To determine the degree which varying volume of the apparatus will have on the rise time to reach peak pressure will use tape to cover the wells of the injury apparatus to demonstrate a volume decrease. The need to decrease the volume is important because it can demonstrate that if have an overall effect to the driving force of air to reach peak pressure at a faster rate. Since the Penn Model only uses a one well injury apparatus, the volume involved in comparison to the volume of the 24 well injury apparatus is many times smaller. As a result, the Penn Model has the ability to reach a higher peak pressure at a lower input reserve pressure. Data taken from an injury apparatus of $0.3in^3$, this volume is derive from the dimensions indicated in Figure 3.12, will be compared with a 5.80 in^3 (Figure C.1) injury apparatus, both having the same setup as show in Figure 3.14b, to evaluate the effect that volume imposes to the acquired pressure.

It is also important to assess whether having a silicone membrane with the aluminum plate, with 24 slits at 0.25" width corresponding to the 24 wells cell culture plate, will have any affect on the rise time and peak pressure.

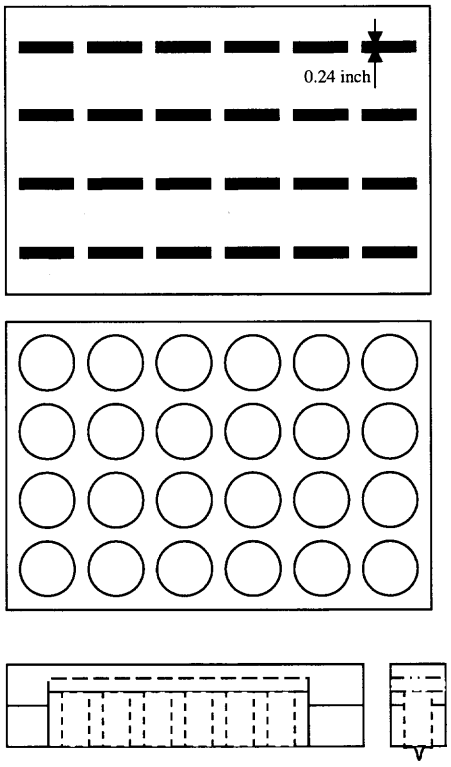

Figure 3.15 (a) 24 slits Aluminum Plate (b) Corresponding 24 Injury Wells (c) Deformation of the silicone membrane with the application of the 24 slits Aluminum Plate.

Therefore, data from the actual injury apparatus with the silicone membrane at 40 psi and 30 ms will be taken and compared with the data from the 24 wells injury plate with the solid bottom enclosure. This arbitrary set of parameters, 40 psi and 30 ms, will be consistently used for comparison between the different apparatus setups, such as those shown in Figure 3.13 and 3.15.

Finally, the last set of data will be collect to evaluate pressure distribution inside the multi-well injury apparatus as air enters its vicinity. A nine-point test will be use for this test. The cover manifold of the injury apparatus for the 24 well plates contains 9 points having screw holes of ¼" hex length, in which the EPX sensor can attach to. These nine points are located in different positions relative to the 24 well plates (Figure 3.16).

Data for each of the points will be collected at a constant pressure of 40 psi and 30 ms. Graphical analysis and statistical analysis will be used to evaluate the air distribution.

Figure 3.16 Top plate manifold of the multi-well injury apparatus, having 9 points for sensor insertion to test pressure at each location.

3.3 Statistical Analysis of Collected Data

All the acquired data will be analyze using Minitab 15 statistical software. A 1 sample t-test will be use to determine consistency and repeatability of the data. Construction of a boxplot will be used to indicate the difference between the apparatus setups and volume difference. This will illustrate what design parameters have a greater effect on the apparatus design.

CHAPTER 4

RESULTS

The automated multi-well neural injury device (NJIT Model) aims to replicate the pressure curve induced by the Penn Model. When comparing the data collected from both models, shown in Figure 4.1, the slope of the rise time is very similar. The major difference is the peak pressure (venting portion of the curve is neglected). The difference in the peak pressure stems from the difference in the volume between the two models. Later in this chapter, the effects of volume will be discussed and presented. In this chapter it will go through the results of the data analysis from automated multi-well neural injury device to evaluate the efficiently and accuracy of the rise time and peak pressure as air is release into the injury apparatus, for use as an *in vitro* model for TBI.

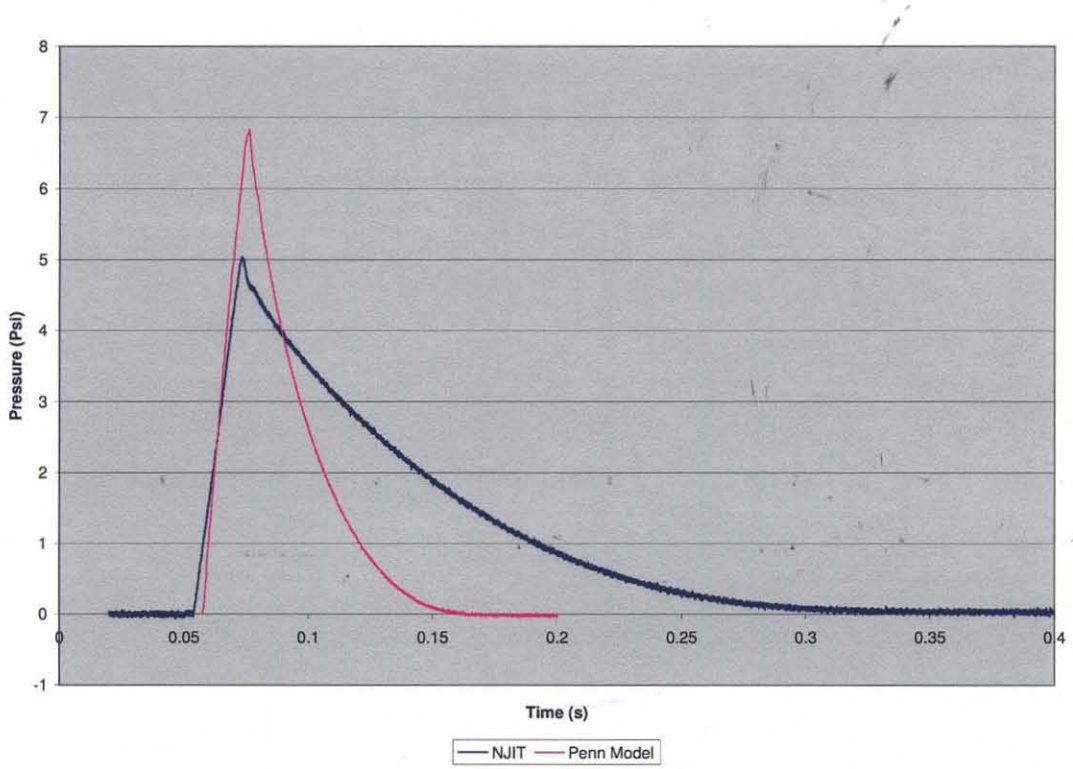

Figure 4.1 Graphical comparison between the data obtained from the Penn Model to the data obtained from the NJIT model (24 well injury apparatus – 5.80 in^3) at 80 psi and 20 ms.

4.1 Timing Resolution of the Series 9 Valve

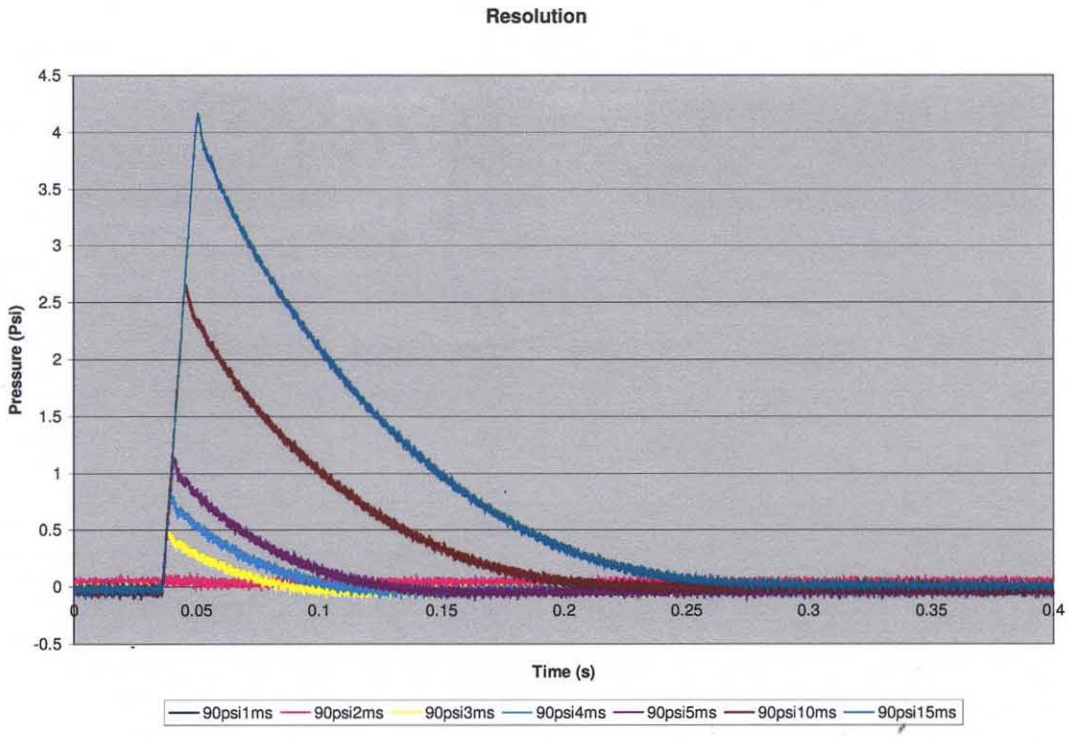

Figure 4.2 Comparing the decreasing input time to evaluate the resolution of the series 9 valve. This graph shows that opening time of 3 ms is the maximum resolution.

The series 9 3-way solenoid valve can open and close within a 5-6 ms time interval. The data collected using the software program has a constant reserve input pressure of 40 psi and the opening time for the series-9 valve is reduced from 20 ms to 1ms. If the pressure curves remain the same after a specific valve opening time, then the maximum resolution will be determined. According to the graph in Figure 4.2, after 3 ms opening interval, the pressure curved obtained for 3 ms or less remain flat. The data in Figure 4.2 is obtained using the dummy volume with 2 inch tube length and 0.25 in diameter going into the close volume.

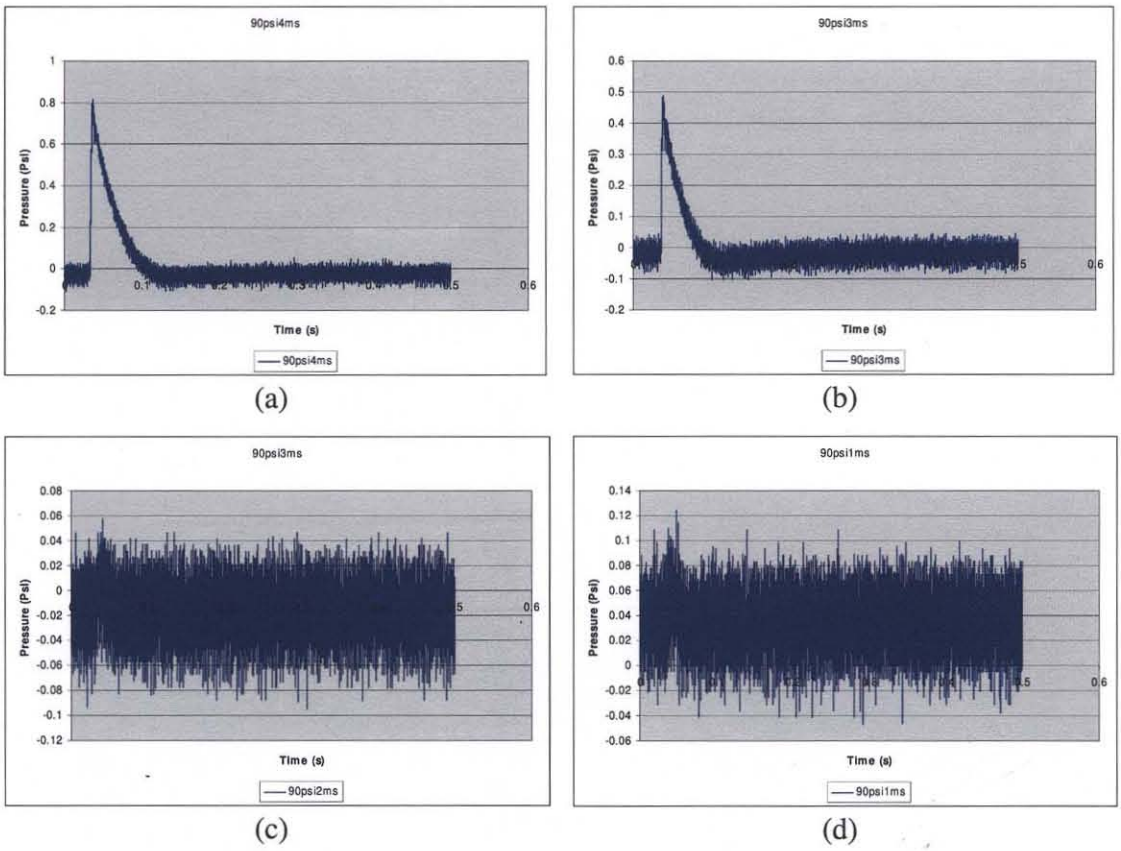

Figure 4.3 Peak Pressure at (a) 90psi and 4 ms, (b) 90 psi and 3 ms, (c) 90 psi and 2 ms And (d) 90 psi 1ms.

The four graphs shown in Figure 4.3 are from data taken from the 24 well apparatus and it clearly illustrate that after 3 ms, any data taken with a valve opening of 2ms or less will remain constant. There are two reasons that may explain this situation. The first reason may stem from the fact that the valve actually can open for 1 ms, but the air that enters into the tube leading to the dummy apparatus loss its driving force to enter into the close volume, dummy apparatus. Therefore, the data collected from the EPX sensor remained at 0 Psi. The second reason may stem from the fact that the valve did not open at all, therefore no air had entered into the apparatus. Based on the specification of the series 9 valve, capable of opening and closing with 5-6ms, the second reason is the most valid. The 2 inch tube leading into the dummy apparatus may not produce enough obstruction

to decrease air driving force to zero. However, in the later section of this chapter, the effect of the tubing and volume will be further analyzed to assess its role in the pressurization of the injury apparatus.

4.2 Consistency and Repeatability

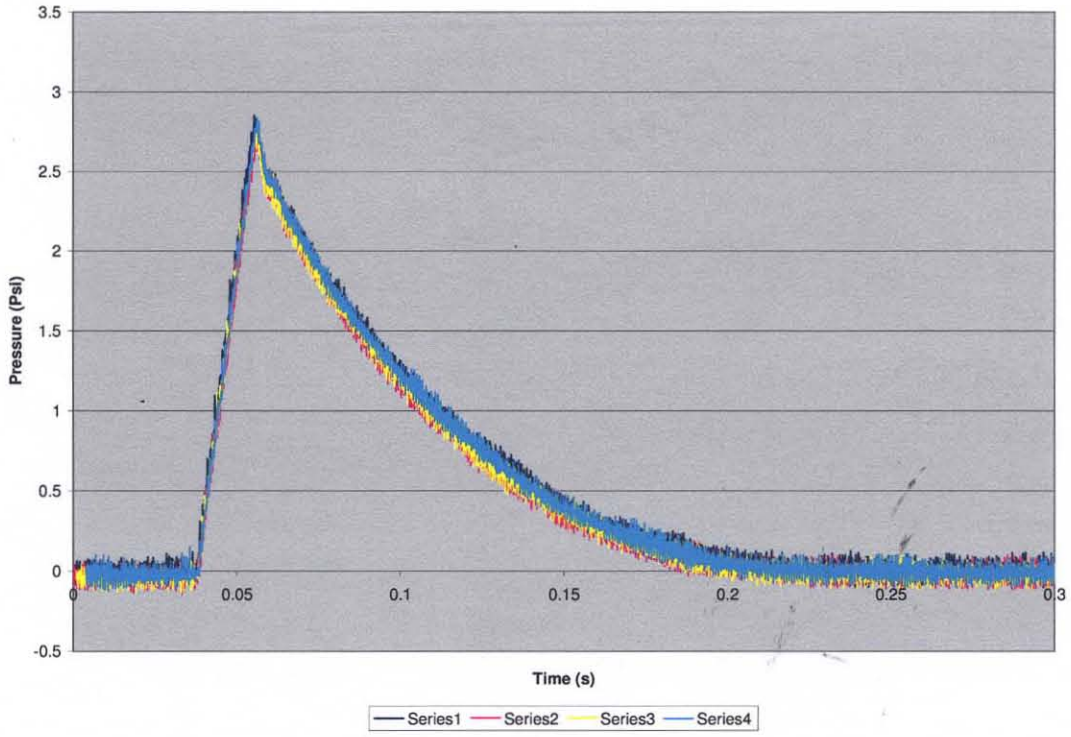

Figure 4.4 Graphical analysis of four consecutive data sets collected for a 40 psi input pressure and 20ms of input time for series 9 valve.

One of the objectives for the automated multi-well neural injury device is to collect data with accuracy, consistency and repeatability in order to accomplish controllability. The data collected in Figure 4.4 is based on a 40 Psi pressure (2V) at 20 ms valve opening time. There are ten sets of data collected consecutively having the same parameters. However, in Figure 4.4, it illustrates only 4 sets of data to show graphically that the data has the same slope, same rise time and peak pressure. Statistical analysis of this particular set of data is based on their peak pressure, an indication of the maximum strain from the

deformation of the silicone. The peak pressures were analyzed using a 1-sample t-test and the results shows a standard deviation of 0.07. This is an indication that the data is relatively consistent with each other. In table 4.1, it shows the results from a 1 sample t-test illustrating that the standard deviation is very low demonstrating both consistency and repeatability among the different data sets.

Samples Type	Sample Size	Standard Deviation
40 Psi / 20 ms	10	0.0720
40 Psi / 30 ms	10	0.0453
40 Psi / 40 ms	10	0.0666
50 Psi / 20 ms	10	0.0493
60 Psi / 20 ms	10	0.0342
70 Psi / 20 ms	10	0.0393

Table 4.1 Statistical Analysis of data consistency at a 95% Confidence Interval.

Due to the high consistency and accuracy in which the acquired data had demonstrated, controllability of the pressure needed for the injury device can be achieved. In Figure 4.5 and Figure 4.6, they are graphs of pressure ramp up at constant valve timing. The valve timing is associated with the time in which peak pressure is reach. It illustrated that the input pressure have a significant effect on the driving force of air to the injury apparatus as indicated by the change in slope in Figure 4.6. In Figure 4.5, although it looks like all the curves have the same slope, but that is not the case. Since the timing of 5 ms is soo small, it is difficult to see the small change in slope as in Figure 4.6. With the appropriate tuning between the input pressure and valve opening time, the desired pressure for the neural injury can easily be obtained.

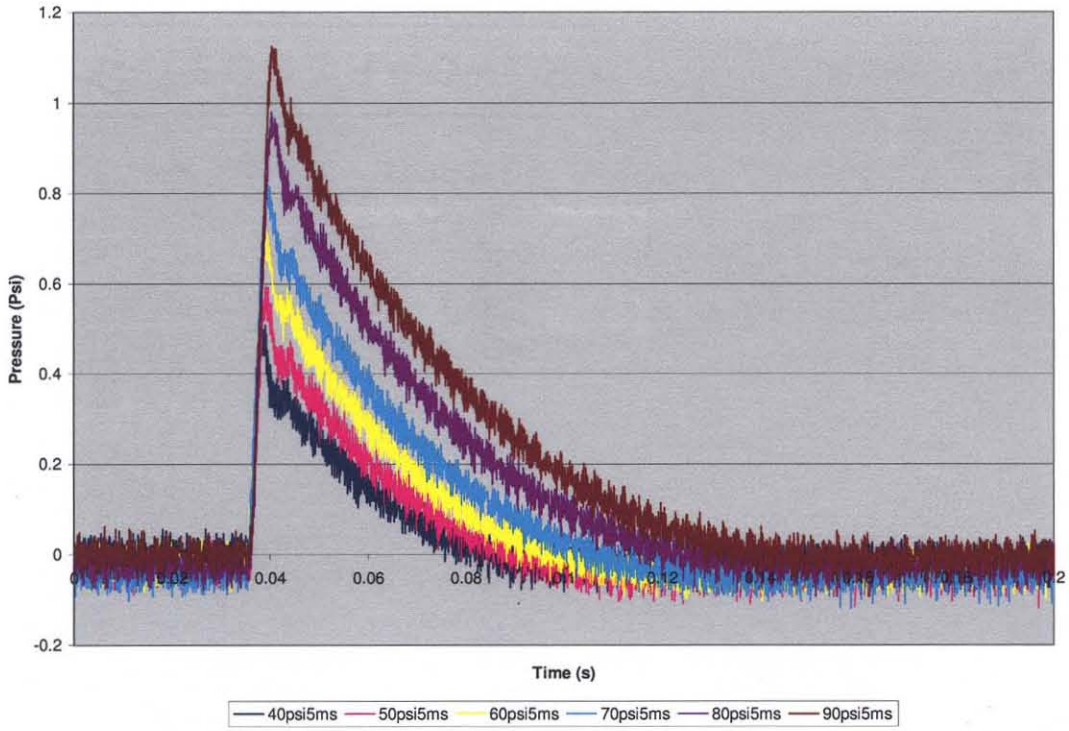

Figure 4.5 Ramping up the pressure from 40 psi to 90 psi with a constant valve timing of 5 ms.

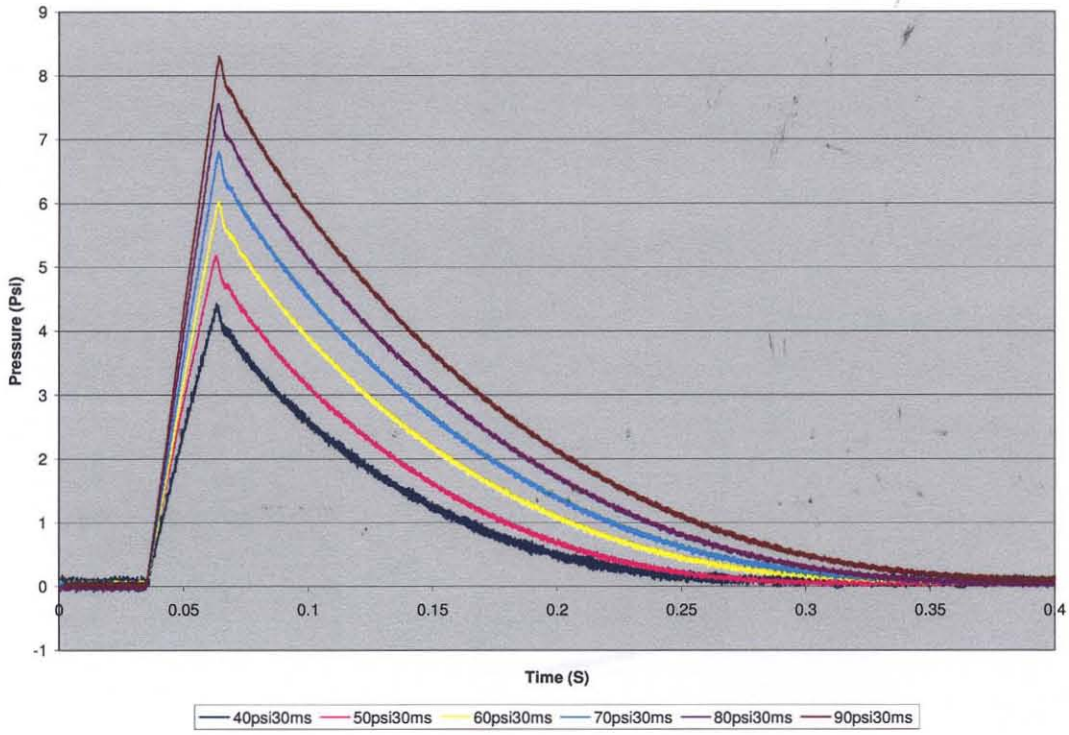

Figure 4.6 Ramping up the pressure from 40 psi to 90 psi with a constant valve timing of 30 ms

Additionally, in Figure 4.7 it illustrates a graph of the resulting peak pressure in accordance to input pressure and variation in timing. Therefore, with proper tuning of the input pressure and valve opening time, high controllability of the desire pressure can be obtained.

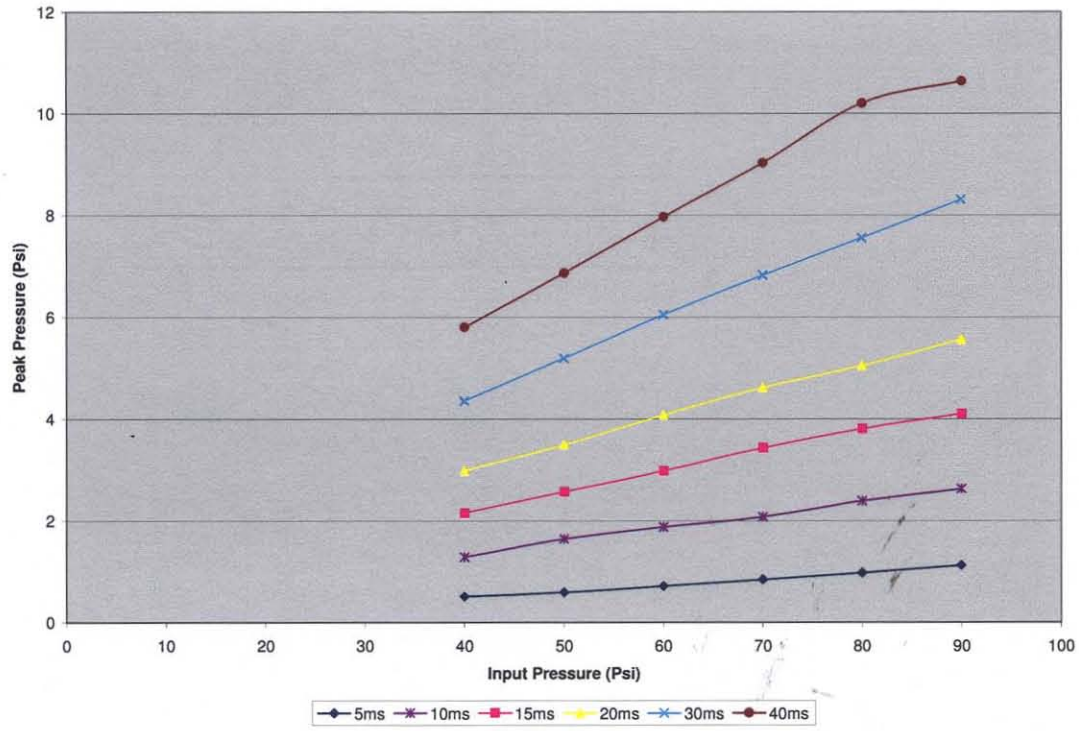

Figure 4.7 Peak Pressure Trend based on Input Pressure and Valve Timing.

4.3 Dummy Volume vs. Injury Apparatus

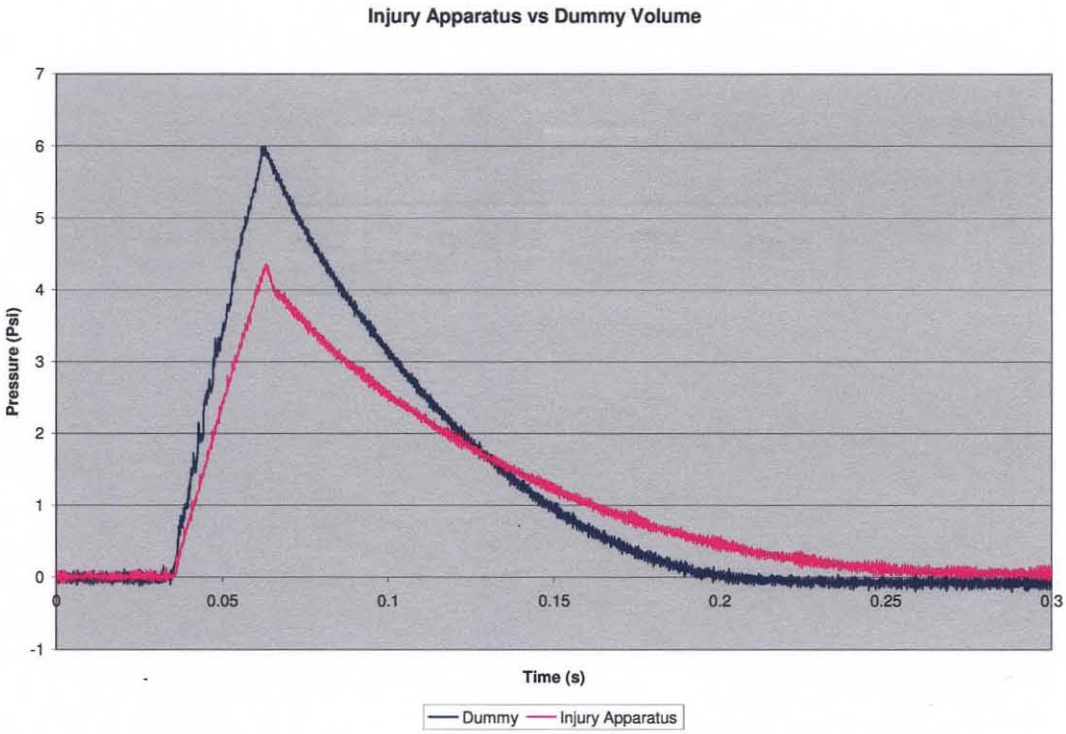

Figure 4.8 Graphical evaluation between the dummy volume setup and actual injury apparatus setup to see the effect of the multiple tubing have on the rise time and peak pressure.

The results of the test between the dummy volume setup and the actual injury apparatus setup is to illustrate how much interference the multiple tubing has on pressurization of the multi-well neural injury apparatus. A constant pressure of 40 Psi and 30 ms valve opening time is used. From Figure 4.8, it can be seen that there is a decrease in the pressure rise time in the injury apparatus compared to the dummy volume; this is indicated by the slope. Additionally, comparing the peak pressure of the dummy volume and the injury apparatus, there is a significant pressure difference. This difference may be due to the lose of air as it is being expose to more volume, from multiple tubing, leading to the injury wells. Therefore, in the design of the apparatus setup, eliminating the amount of tubes used is an important factor in the rise time. Eliminating unnecessary tubing will decrease volume and losses in the driving force of air going into the 24 well

injury apparatus and increase slope and peak pressure obtained. In this example, at a constant pressure of 40 psi, by decreasing the amount of obstruction, it can produce a peak pressure greater than 4.36 psi at 30 ms can be obtained.

4.4 The Effect of Lowering the Volume

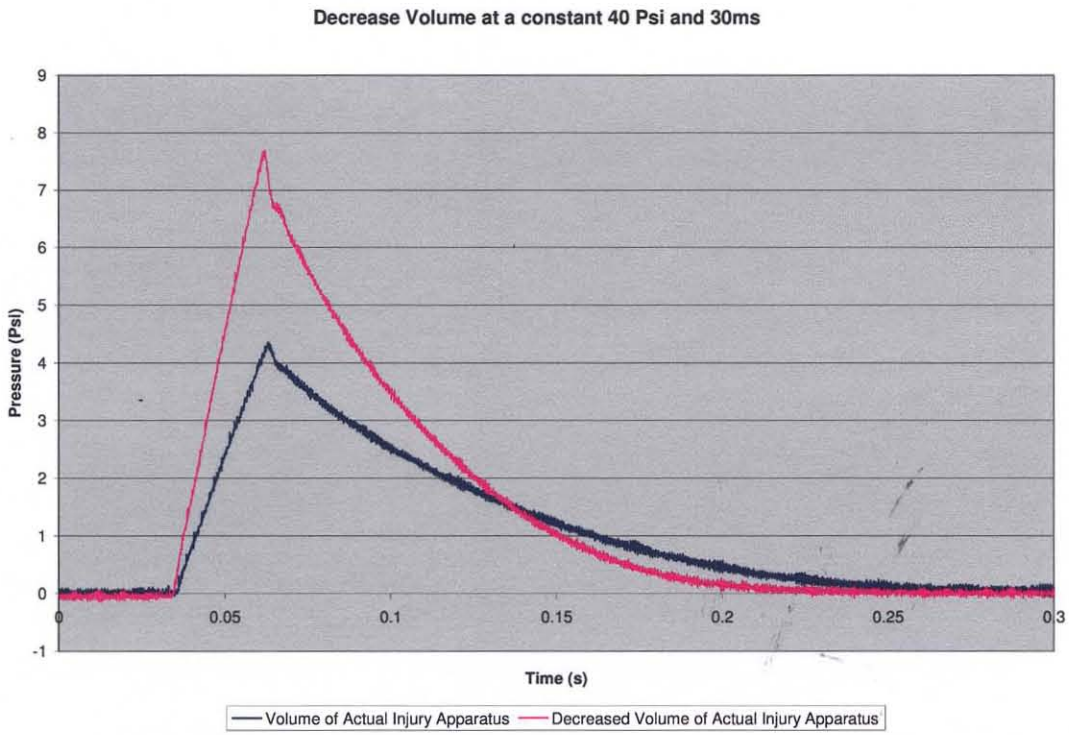

Figure 4.9 This graph illustrates that by decreasing the volume it have a direct effect to to the slope and peak pressure of the injury apparatus.

The volume of the injury apparatus havs a direct effect on rise time and peak pressure of produced by the injury apparatus. The result in Figure 4.9 is obtained by first collecting data using the 24 well injury apparatus. Tape was used to block the wells of the 24 well plates to achieve a smaller volume of 0.3 in^3 (Figure 3.2). Data was collected for the smaller volume to see its effect on the rise time and peak pressure. The results demonstrate that by decreasing the volume, same the driving force allowed it to reach a higher peak pressure than the larger volume. Since the volume is smaller, the time it takes

to distribute the air throughout that smaller volume takes less time which explains the steeper slope.

4.5 Injury Apparatus with Silicone Membrane vs. Injury Apparatus without Silicone Membrane

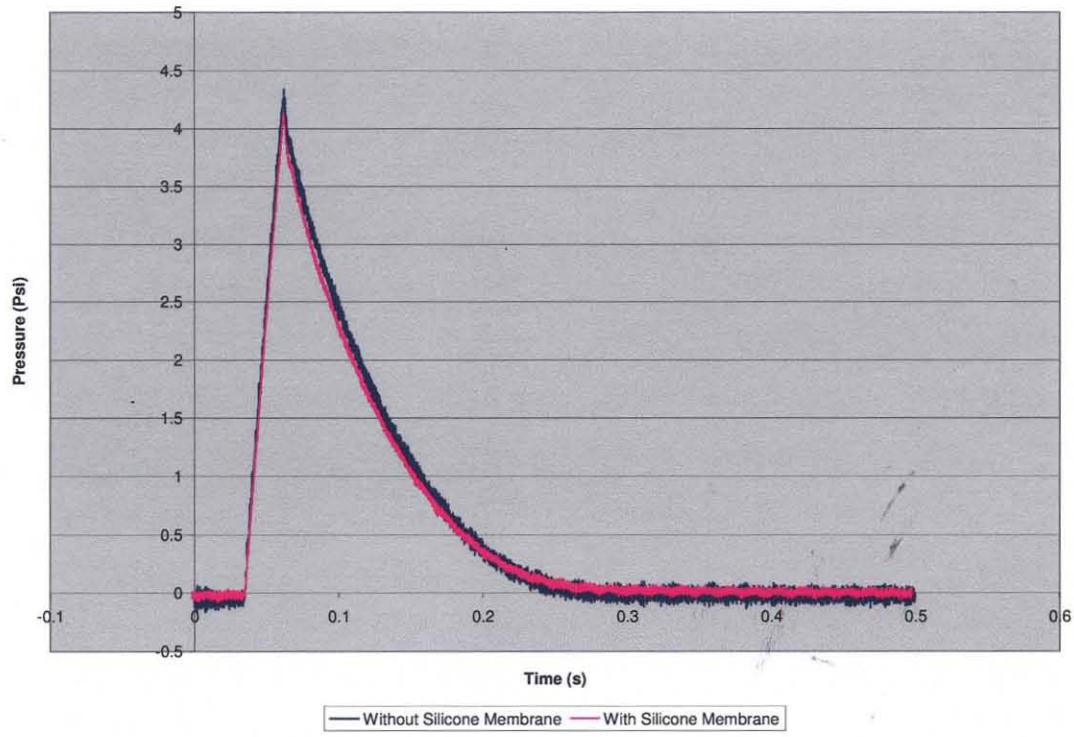

Figure 4.10 Pressure data take at 40psi and 30ms valve timing.

Many sets of data that was shown in the previous few sections of this chapter had been taken from a 24 well injury apparatus in which it contains a rigid plastic bottom enclosure. In the actual neural injury device, the 24 well injury apparatus has a sheet of silicone membrane attached to the bottom, in which the cells are cultured. The actual injury design also contains an aluminum plate with 24 of the quarter inch wide slit corresponding to the center of the circular wells of the injury apparatus. The slit is where uniaxial stretch of the neural cells take place. When comparing the apparatus with the

solid enclosure and the apparatus with the silicone membrane attached using power anaylsis, the output data shows no significant difference as illustrated in Figure 4.10. In the boxplot below (Figure 4.11), it shows a slight difference in peak pressure between the two design because the silicone membrane is elastic and the volume increased slightly as air passes through, decreasing the peak pressure obtained. However, the difference between the two apparatus does not varied so much that one can say they are different.

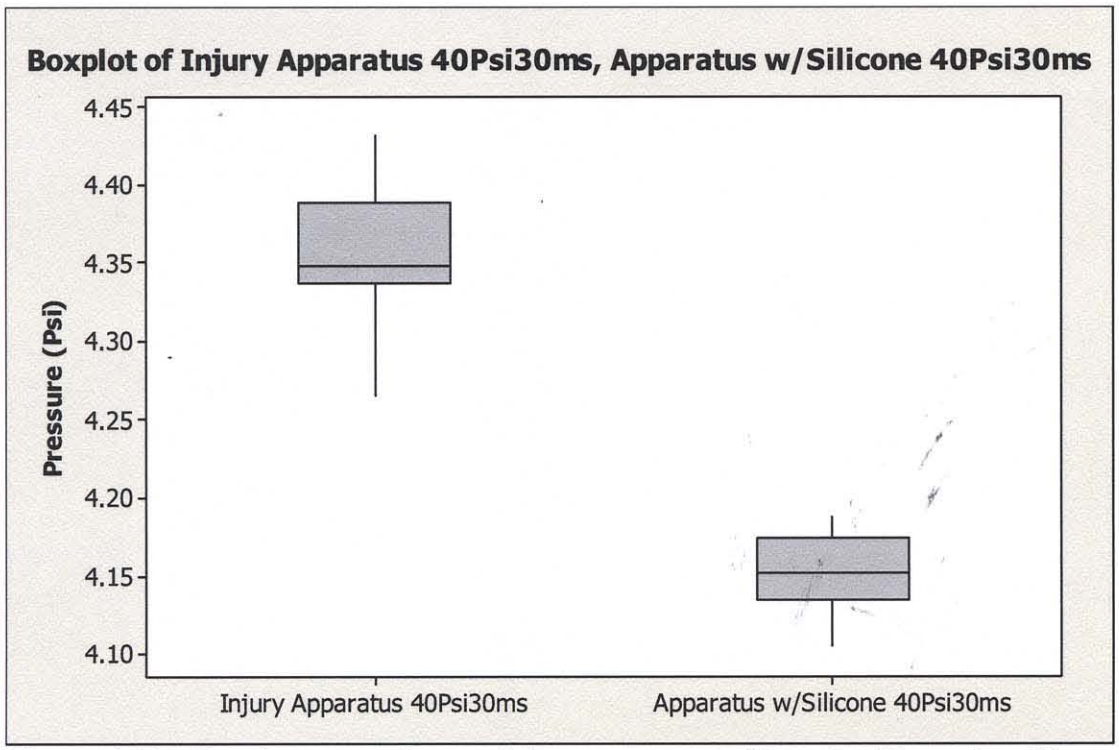

Figure 4.11 Boxplot comparing an injury apparatus with and without the silicone membrane.

4.6 Air Distribution within the Injury Apparatus

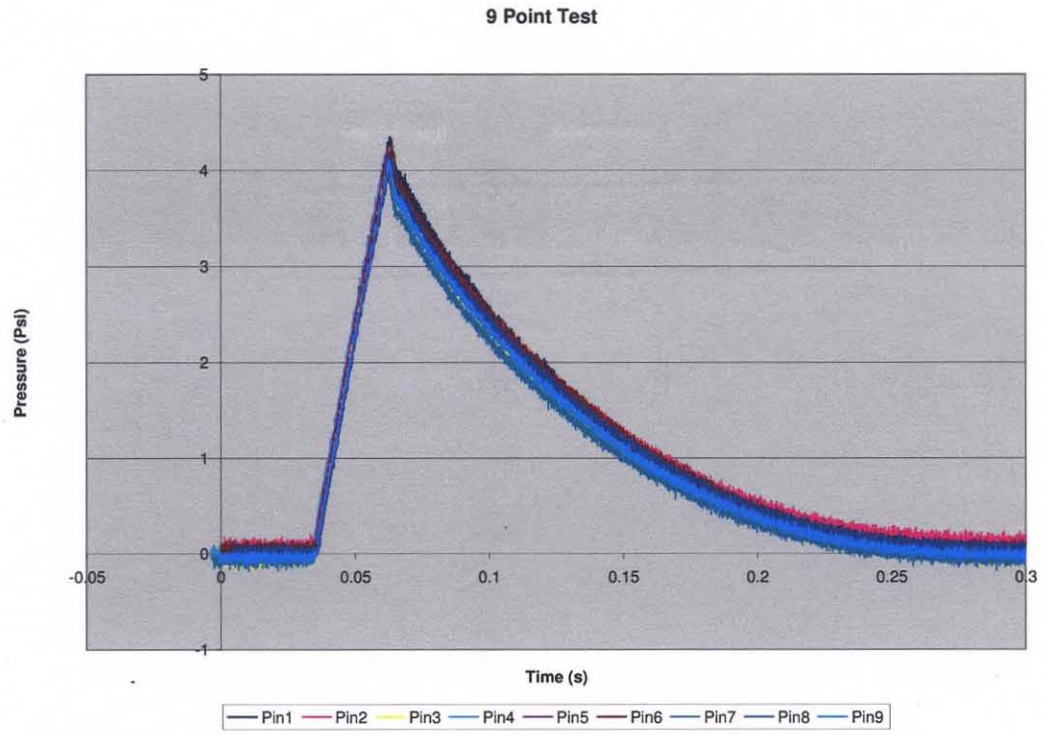

Figure 4.12 This graph illustrates consistency of air distribution with the 24 well Apparatus at 40 psi and 30 ms.

The result of the 9 point test for air pressure distribution is conducted using the 24 well apparatus with the solid bottom enclosure. Since the results of the previous section shows that the data obtained from both design has no significant difference, the results from this test can be applied to the actual injury apparatus using the silicone membrane. The above graph shown in Figure 4.12 is a 9 point test to determine the air flow dynamics within the injury wells. The results indicate that all the wells are able to reach similar peak pressure with the same rise time having a standard deviation of 0.1060 at a 95% confidence interval. Although the peak pressure has a higher deviation than the data is not as consistent as the data shown in Table 4.1, the pressure pulses are very consistent. The reason that the standard deviation is higher in this data set was because it is collected at different locations. However, these results are important because it demonstrates that all

24 wells are able to be exposed to the similar pressure, injuring all the cultured neurons at the same time and magnitude. This will eliminate any variability in the collected data and enable high throughput experiments for studying these injured cells.

4.7 Hardware Time vs. Software Time

Prior to switching to a new DAQ card and changing the timing control to hardware time, software timing was used. From the data collected using both timing techniques, the software based timing is less superior to hardware timing in terms of consistency in controlling the solenoid valve. A 1 sample t-test is employed to assess the data collected via software timing and the result show in the figure below.

One-Sample T: Software Time for 40Psi 20ms

Variable	N	Mean	StDev	SE Mean	95% CI
Software Time for 40Psi	10	1.9000	0.1911	0.0604	(1.7633, 2.0367)

Figure 4.13 Using Minitab to perform a one-sample T-test of the data collect using software timing.

When comparing to the data in Table 4.1 to that of Figure 4.13, the data consistency is better using hardware timing. Therefore, hardware timing outperforms software timing.

CHAPTER 5

CONCLUSION

According to the results presented in chapter 4, the automated multi-well neural injury device is able to mimic the condition of neurons during TBI. The collected data indicated that it is comparable to that of a blast head injury pressure curve. In addition, the slope of the rise time is similar to that produced by the Penn Model.

Although the data indicate that the software program accomplishes its entire objective, the design of the injury apparatus can be modified in optimize the flow dynamics. For example, by decreasing the volume of the apparatus and eliminating tube length, it will increase the slope of the rise time and peak pressure. Currently, the device is able to reach 7 psi pressure inside the injury apparatus with an input pressure of 80 psi and 20 ms opening time of the solenoid valve. However, with the proper modification, it may reach a peak pressure of 7 psi at a lower reserve pressure within the 20 ms opening time. In Figure 5.1, it is a boxplot between the difference in tubing, and volume in comparison to the current injury apparatus setup. It illustrates that decreasing volume have a more significant effect to the peak pressure as compared with decreasing tube length. Also, having a silicone membrane instead of a solid bottom had no significant effect on the rise time and peak pressure.

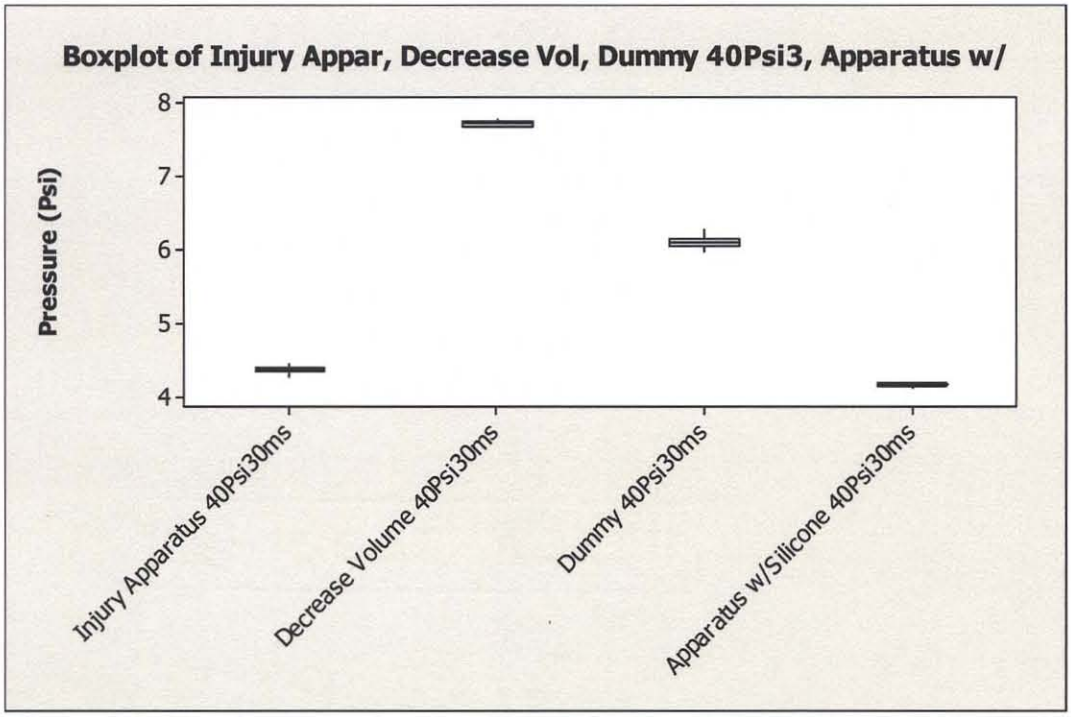

Figure 5.1 Boxplot comparing the effects of tubing design and volume in the injury apparatus design.

Furthermore, using hardware time instead of software time creates a control interface with better performance. The results in chapter 4 had illustrated that the data obtained from software timing have a significantly higher standard deviation as to those obtained via hardware timing. Therefore, hardware timing outperformed software timing in terms of controllability, accuracy, consistency and repeatability.

Although this system is reliable in its performance and control in accordance to the obtained result, there are some additional design modifications required. One of the objectives of this research is to be able to reach 7 psi of pressure within 5 ms valve timing. This objective was not met because the hardware components are unable to handle more than 100 psi of input reserve pressure. In Figure 5.2, it is a graph of 90 psi of input pressure at 5 ms and the pressure was only able to reach is only 1.12 Psi of peak pressure. Therefore, this demonstrates that a large amount of input pressure is needed to create a driving force to reach the peak pressure at 5 ms valve opening time.

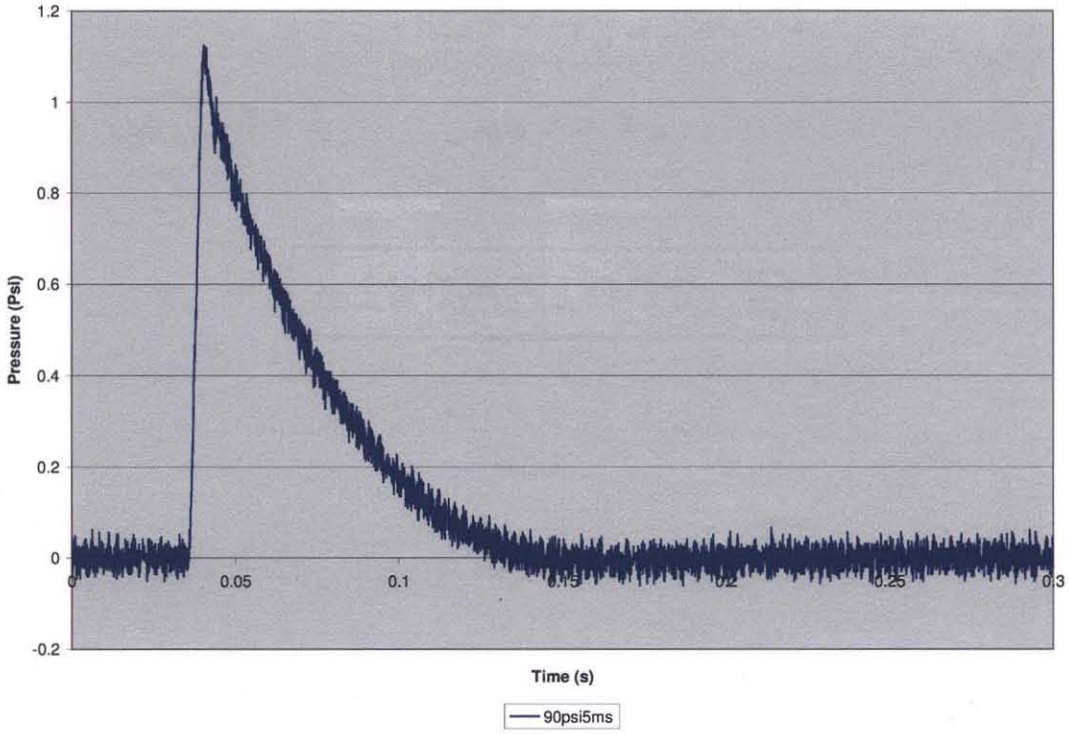

Figure 5.2 Data from an input pressure of 90 psi for 5 ms.

Another way the design can be modified is to overdrive the solenoid valve to open completely to release air at its full capacity at the specify time. According to Figure 4.7, at 5 ms, the solenoid valve does not seem to open completely. Another way to approach this issue is to add another solenoid valve to increase the amount of air going through the valve at the specify time interval.

Nevertheless, this current system is able to accommodate a high throughput experiments for 24 wells of cultured neurons and induced injury to all these cells at the same time with accuracy and consistency. Additionally, the injury induced can be controlled fairly easily through varying the input pressure and the valve opening time. Therefore, this system is a very reliable system as an in vitro model for mimicking different forms of TBI.

APPENDIX A

HARDWARE SCHEMATIC

This is the complete circuit layout of the hardware component that controls the injury device.

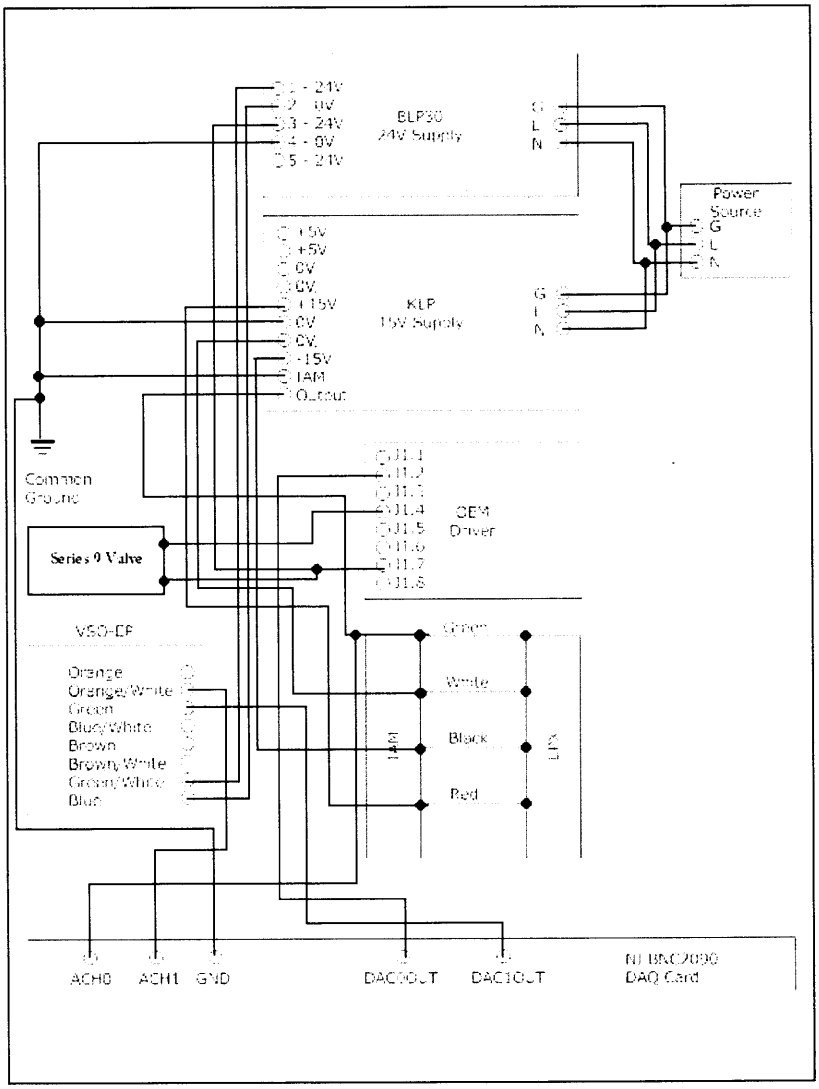

Figure A.1 Circuit Schematic of the connections between the hardware components.

APPENDIX B

CALCULATION OF THE FLOW DYNAMIC

The calculation performed here is based on Bernoulli's Equation for compressible flow.

It is to evaluate the volume of air flow going into the injury apparatus.

P_1 = 100 psi (lb_f/in^2) or 14400 lb_f/ft^2
P_2 = 10 psi (lb_f/in^2) or 1440 lb_f/ft^2
D_1 = 0.021 ft
D_2 = 0.0097 ft
ρ = 0.0796 lb_m/ft^3

Equation: $$\boxed{P_1 - P_2 = 16Q^2\rho\left(\frac{1}{\pi^2 D_1^4} - \frac{1}{\pi^2 D_2^4}\right)}$$

Rearrange: $$Q = \sqrt{\frac{\pi^2\left(P_1 - P_2\right)\left(D_1^4 - D_2^4\right)}{16\rho}}$$

$$Q = \sqrt{\frac{\pi^2\left(\frac{14400lb_f}{ft^2} - \frac{1440lb_f}{ft^2}\right)\left(\frac{32.174lb_m ft}{s^2 lb_f}\right)\left([0.021ft]^4 - [0.0097ft]^4\right)}{16\left(0.0796lb_m / ft^3\right)}}$$

Q = 0.7741 ft^3/s

What is the volume after 20 ms?

Volume = (0.7741 ft^3/s) (0.02s) = 0.015 ft^3

Using this method, here is the generated graph:

P_1 = 80 psi (lb_f/in^2) or 11520 lb_f/ft^2
P_2 = 7 psi (lb_f/in^2) or 1008 lb_f/ft^2
D_1 = 0.021 ft
D_2 = 0.0097 ft
ρ = 0.0796 lb_m/ft^3

$$Q = \sqrt{\frac{\pi^2\left(\frac{11520lb_f}{ft^2} - \frac{1008lb_f}{ft^2}\right)\left(\frac{32.174lb_m ft}{s^2 lb_f}\right)\left([0.021ft]^4 - [0.0097ft]^4\right)}{16\left(0.0796lb_m / ft^3\right)}} = 0.6975 ft^3/s$$

$$V_{5ms} = \frac{0.6975 ft^3}{s} \times \frac{(12in)^3}{1ft^3} \times 0.005 = 6.03in^3$$

APPENDIX C

VOLUME CALCULATION OF THE INJURY WELLS

This is the calculation of the volume of a 24 well cell culture plate for the neural injury apparatus.

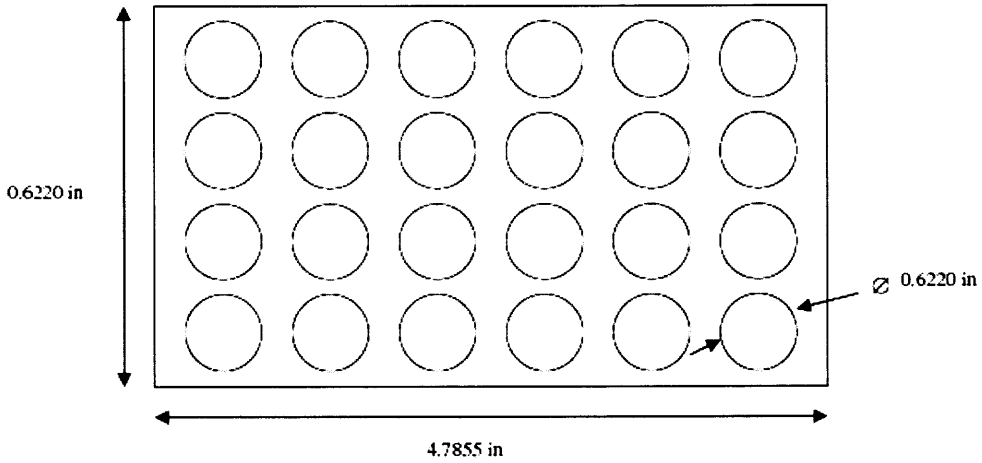

Thickness (D): 0.7555 in
Diameter (Ø): 0.6220 in
Length (L): 2.9570 in
Width (W): 4.7855 in

$$V_{Wells} = \pi r^2 h$$

$$V_{Wells} = \left[\pi\left(\frac{0.6220in}{2}\right)^2 (0.7555in)\right] = 0.2296in^3$$

$$V_{24Wells} = 0.2296in^3 \times 24 = 5.51in^3$$

$$\text{Re}cess\_Space = 0.1in$$

$$V_{recess\_space} = 0.1in \times 4.7855in \times 0.6220in$$

$$V_{Total} = 5.81in^3$$

Figure C.1 Calculation of the volume occupied by a 24 well cell culture plate used in the neural injury apparatus.

APPENDIX D

TABLE OF THE FLOW DYNAMIC

This table is based on the calculation from the derived equation from Bernoulli's Equation for compressible flow. These calculated data is based on an orifice size of 0.116" in diameter.

P1 (psi)	P2 (psi)	P1 (lbf/ft^2)	P2 (lbf/ft^2)	D1 (ft)	D2 (ft)	ρ (lbm/ft^3)	Q (ft^3/s)	Volume @ 20ms (in^3)	Volume @ 10ms (in^3)	Volume @ 5ms (in^3)
0	7	0	1008	0.021	0.0097	0.0796	0	0	0	0
20	7	2880	1008	0.021	0.0097	0.0796	0.294198464	10.16749891	5.083749455	2.541874727
30	7	4320	1008	0.021	0.0097	0.0796	0.391320539	13.52403781	6.762018906	3.381009453
40	7	5760	1008	0.021	0.0097	0.0796	0.468733177	16.19941861	8.099709307	4.049854653
50	7	7200	1008	0.021	0.0097	0.0796	0.535060575	18.49169349	9.245846744	4.622923372
60	7	8640	1008	0.021	0.0097	0.0796	0.594027649	20.52959553	10.26479777	5.132398883
70	7	10080	1008	0.021	0.0097	0.0796	0.647647956	22.38271336	11.19135668	5.59567834
80	7	11520	1008	0.021	0.0097	0.0796	0.697156297	24.09372163	12.04686082	6.023430408
90	7	12960	1008	0.021	0.0097	0.0796	0.743374691	25.6910293	12.84551465	6.422757326
91	7	13104	1008	0.021	0.0097	0.0796	0.747839444	25.84533117	12.92266558	6.461332792
92	7	13248	1008	0.021	0.0097	0.0796	0.752277699	25.99871727	12.99935863	6.499679317
93	7	13392	1008	0.021	0.0097	0.0796	0.756689923	26.15120372	13.07560186	6.537800931
94	7	13536	1008	0.021	0.0097	0.0796	0.761076568	26.30280617	13.15140309	6.575701543
95	7	13680	1008	0.021	0.0097	0.0796	0.765438074	26.45353982	13.22676991	6.613384955
97	7	13968	1008	0.021	0.0097	0.0796	0.774087366	26.75245936	13.37622968	6.688114841
98	7	14112	1008	0.021	0.0097	0.0796	0.778375971	26.90067357	13.45033678	6.725168392
98.1	7	14126.4	1008	0.021	0.0097	0.0796	0.778803533	26.9154501	13.45772505	6.728862525
98.2	7	14140.8	1008	0.021	0.0097	0.0796	0.77923086	26.93021852	13.46510926	6.732554631
98.3	7	14155.2	1008	0.021	0.0097	0.0796	0.779657953	26.94497885	13.47248943	6.736244713
98.4	7	14169.6	1008	0.021	0.0097	0.0796	0.780084812	26.9597311	13.47986555	6.739932775
98.5	7	14184	1008	0.021	0.0097	0.0796	0.780511438	26.97447528	13.48723764	6.74361882
99	7	14256	1008	0.021	0.0097	0.0796	0.782641077	27.04807562	13.52403781	6.762018906
100	7	14400	1008	0.021	0.0097	0.0796	0.786883065	27.19467873	13.59733937	6.798669683

Table D.1 The data from this table is based on the Bernoulli Flow Equation.

APPENDIX E

SOFTWARE BASED TIMING CONTROL PROGRAM

The program uses software time with the USB NI-6009 DAQ Card. In addition, it also contains streaming data acquisition using string function and output it as a binary file.

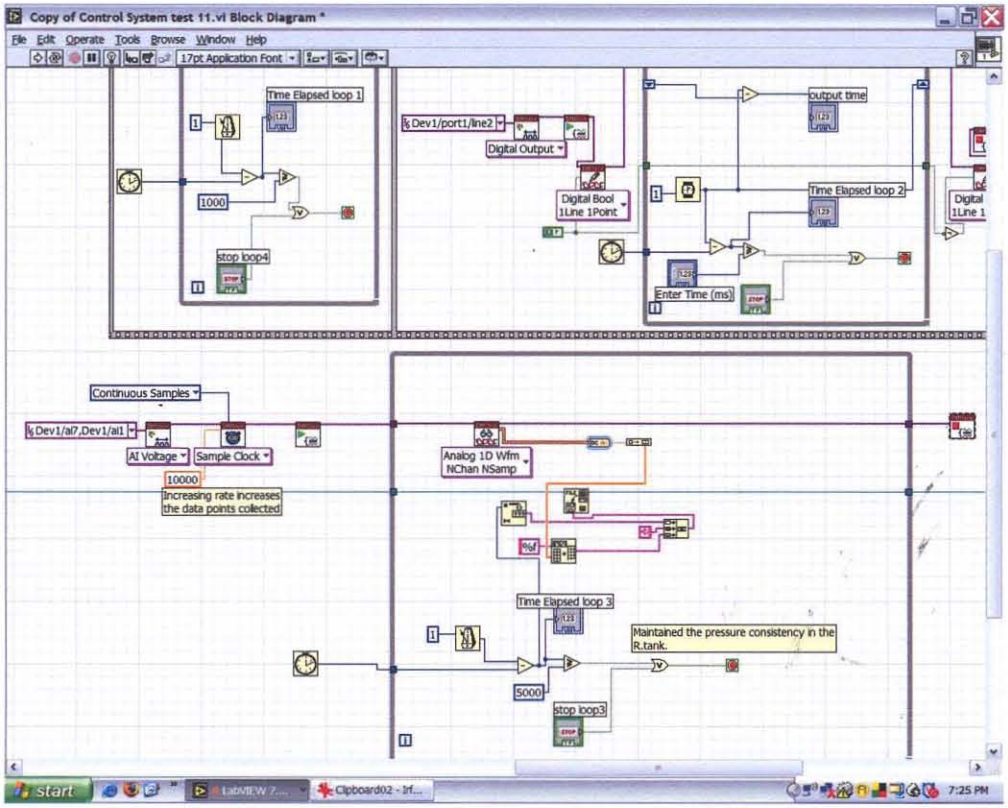

Figure E.1 Illustration of software timing and data acquisition by converting the collected data to string.

APPENDIX F

HARDWARE BASED TIMING CONTROL PROGRAM

The program below uses based timing with the NI BNC 2090 DAQ Card. The task, opening the series 9 valve, is defined prior to initialization via a defined waveform.

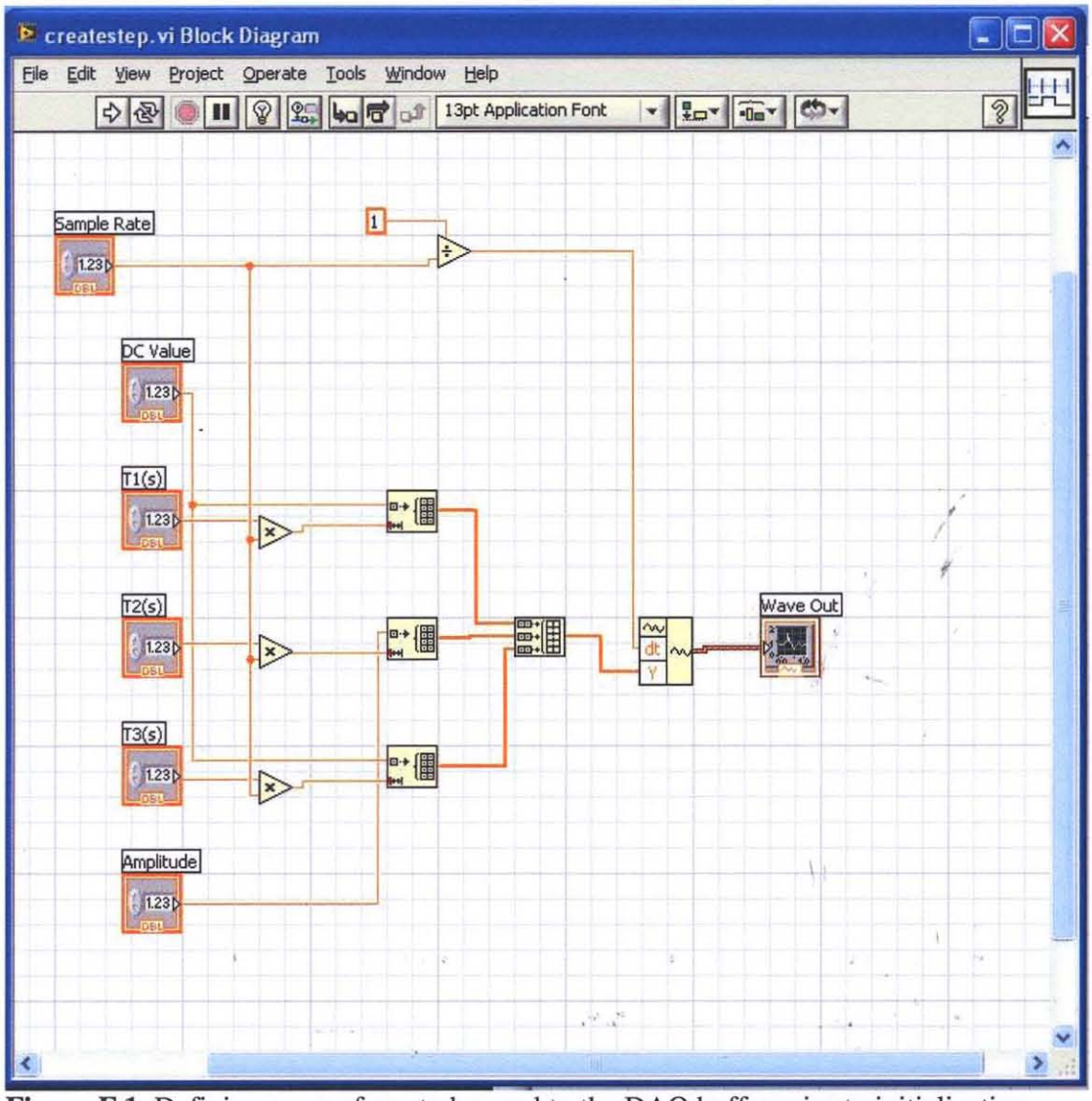

Figure F.1 Defining a waveform to be send to the DAQ buffer prior to initialization.

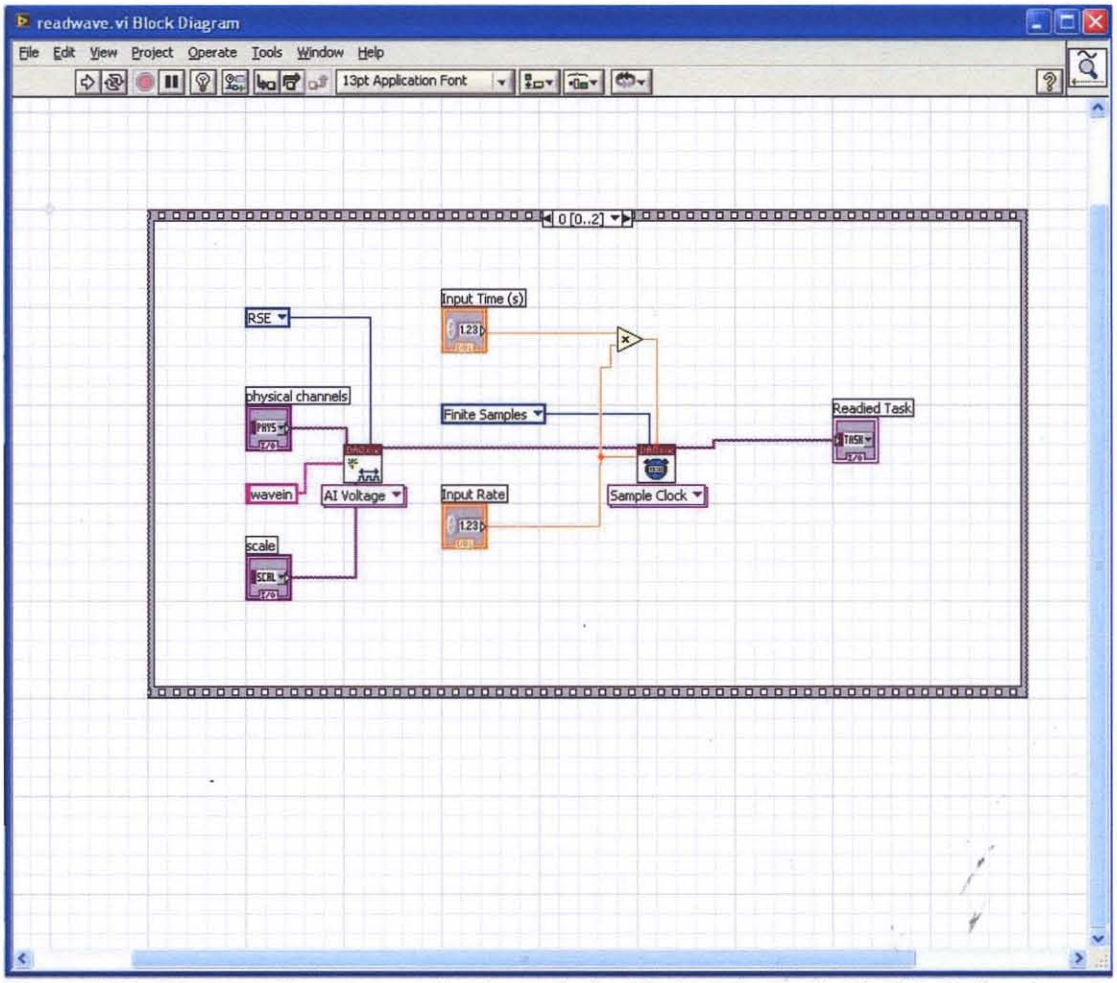

Figure F.2 The waveform instruction is read via this function and downloaded to the DAQ buffer.

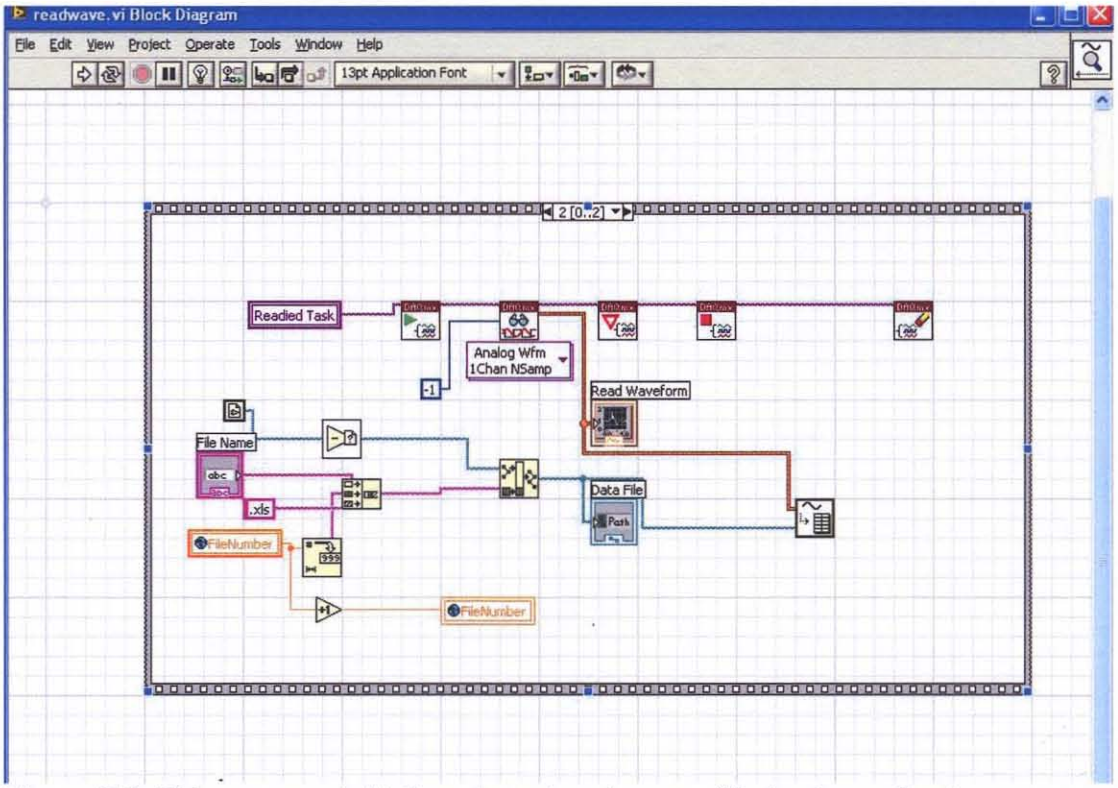

Figure F.3 This sequence initializes the task and creates file for data collection.

REFERENCES

[1] B. J. Pfister, T. P. Weihs, M. Betenbaugh, and G. Bao, "An In Vitro Uniaxial Stretch Model for Axonal Injury," *Annals of Biomedical Engineering,* vol. 31, pp. 589-598, 2003.

[2] D. H. Smith, D. F. Meaney, and W. H. Shull, "Diffuse Axonal Injury in Head Trauma." *J Head Trauma Rehabil.,* vol. 18, pp. 307-316, 2003.

[3] B. J. Pfister, "Multi-Well Neural Injury Device," Newark, NY: New Jersey Institute of Technology, NIH Grant Proposal, 2007.

[4] D. M. Geddes and R. S. Cargill II, "An in Vitro Model of Neural Trauma: Device Characterization and Calcium Response to Mechanical Stretch," *Journal of Biomedical Engineering,* vol. 123, pp. 247-255, June 2001.

[5] B. Morrison III, D. F. Meaney, and T. K. McIntosh, "Mechanical Characterization of an In Vitro Device Designed to Quantitatively Injure Living Brain Tissue," *Annals of Biomedical Engineering,* vol. 26, pp. 381-390, 1998.

[6] Langlois JA , Rutland-Brown W , and T. KE, "Traumatic Brain Injury in the United States: emergency department visits, hospitalizations, and death," Centers for Disease Control and Prevention, National Center for Injury Prevention and Control, Alanta, GA 2006.

[7] M. Smith, "Diffuse Axonal Injury in Adults," *Trauma,* vol. 5, pp. 227-234, 2003.

[8] E. Giugni, U. Sabatini, G. E. Hagberg, R. Formisano, and A. Castriota-Scanderbeg, "Fast Detection of Diffuse Axonal Damage in Severe Traumatic Brain Injury: Comparison of Gradient-Recalled Echo and Turbo Proton Echo-Planar Spectroscopic Imaging MRI Sequences," *American Society of Neuroradiology,* vol. 26, pp. 1140-1148, May 2005.

[9] T. Gennarelli, L. Thibault, R. Tipperman, and et al., "Axonal injury in the optic nerve: a model simulating diffuse axonal injury in the brain," *Journal of Neurosurgery,* vol. 71, pp. 244-253, 1989.

[10] J. A. Wolf, P. Stys, T. Lusardi, D. F. Meaney, and D. H. Smith, "Traumatic axonal injury induces calcium influx modulated by Tetrodotoxin-sensitive sodium channels," *Journal of Neuroscience,* vol. 21, pp. 1923-1930, 2001.

[11] H. Metz, J. McElhaney, and A. Ommaya, "A comparison of the elasticity of live, dead, and fixed brain tissue," *Journal of Biomechanics,* vol. 3, pp. 453-458, 1970.

[12] B. Morrison III, K E. Saatman, D. F. Meaney, and T. K. McIntosh, "In Vitro Central Nervous System Models of Mechanically Induced Trauma: A Review," *Journal of Neurotrauma,* vol. 15, pp. 911-927, 1998.

[13] J. H. Lucas and J. A. Wolf, "In vitro studies of multiple impact injury to mammalian CNS neurons: prevention of perikaryal damage and death by ketamine " *Brin Res,* vol. 543, pp. 181-193, 1991.

[14] S. S. Margulies, "Biomechanics of traumatic coma in the primate." Ph.D Dissertation, Philadelphia, PA: University of Pennsylvania, 1990.

[15] S. S. Margulies, K. A. Willoughby, S. Liang, and E. F. Ellis, "Physical model simulations of brain injury in the primate," *Journal of Biomechnics,* vol. 23, pp. 823-836, 1996.

[16] D. F. Meaney, "Biomechanics of acute subdural hematoma in the subhuman primate and man." vol. Ph.D Philadelphia, PA: University of Pennsylvania, 1991.

[17] D. F. Meaney and L. Thibault, "Physical model studies of cortical brain deformation in response to high strain rate inertial loading," in *International Conference on the Biomechanics of Impacts*, Lyon, France, 1990, pp. 215-224.

[18] J. L. Shaffer, M. Rizen, G. J. L'Italien, A. Benbrahim, J. Megerman, L. C. Gerstenfeld, and M. L. Gray, "Device for the Application of a Dynamic Biaxially Uniform and Isotropic Strain to a Flexible Cell Culture Membrane," *Journal of Orthopaedic Research,* vol. 12, pp. 709-719, 1994.

[19] M. Douglas H. Smith, J. A. Wolf, T. A. Lusardi, V. M.-Y. Lee, and D. F. Meaney, "High Tolerance and Delayed Elastic Response of Cultured Axons to Dynamic Stretch Injury," *The Journal of Neuroscience,* vol. 19, pp. 4263-4269, June 1, 1999.

[20] "OEM Valve Driver Data Sheet," Parker Hannifin Corporation, General Valve Operation, New Jersey April 2003.

[21] K. H. Taber, D. L. Waden, and R. A. Hurley, "Blast-Related Traumatic Brain Injury: What Is Known?," *The Journal of Neuropsychiatry & Clinical Neurosciences,* vol. 18, pp. 141-145, May 2006.

[22] *Learn 10 Functions in NI-DAQmx and Handle 80 Percent of Your Data Acquisition Applications*. Retrieved April 2, 2008, from http://zone.ni.com/devzone/cda/tut/p/id/2835

[23] *CT Scan Guidance.* Retrieved April 10, 2008, from http://www.crash.lshtm.ac.uk/ctscan.html

[24] Choudhury, Mridusmita, "Automated Multi-well Neural Injury Device." M.S. Thesis, Newark, NJ: New Jersey Institute of Technology, 2007.